https://doi.org/10.5194/acp-2020-340
Preprint. Discussion started: 18 May 2020

Atmospheric Chemistry and Physics Discussions

Baffin Bay sea ice extent and synoptic moisture transport drive water vapor isotope ($\delta^{18}O$, δD, *d-excess*) variability in coastal northwest Greenland

Pete D. Akers[1], Ben G. Kopec[2], Kyle S. Mattingly[3], Eric S. Klein[4], Douglas Causey[2], Jeffrey M. Welker[2, 5]

1. Institut des Géosciences et l'Environnement, CNRS, Saint Martin d'Hères, 38400, France.
2. Department of Biological Sciences, University of Alaska Anchorage, Anchorage, 99508, AK, USA.
3. Institute of Earth, Ocean, and Atmospheric Sciences, Rutgers University, Piscataway, 08854, NJ, USA
4. Department of Geological Sciences, University of Alaska Anchorage, Anchorage, 99508, AK, USA.
5. Ecology and Genetics Research Unit, University of Oulu, Oulu, 90014, Finland, and University of the Arctic-UArctic

Correspondence to: Pete D. Akers (pete.d.akers@gmail.com)

Abstract

At Thule Air Base on the coast of Baffin Bay (76.51° N 68.74° W), we continuously measured water vapor isotopes ($\delta^{18}O$, δD) at high frequency (1 s^{-1}) from August 2017 through August 2019. Our resulting record, including derived *deuterium-excess* (*dxs*) values, allows for analysis of isotopic-meteorological relationships at an unprecedented level of detail and duration for High Arctic Greenland. We examine isotopic variability across multiple temporal scales from daily to annual, revealing that isotopic values at Thule are determined by five interacting factors: a) local air temperature, b) local marine moisture availability, c) the North Atlantic Oscillation (NAO), d) surface wind regime, and e) land-based evaporation/sublimation. Each factor's relative importance changes in response to seasonal shifts in Thule's environment, largely driven by the sea ice extent in northern Baffin Bay. Winter sea ice coverage forces distant sourcing of vapor that is isotopically light from fractionation during transport and prevents isotopic exchange with local waters. Late spring sea ice breakup triggers a rapid isotopic change at Thule as the newly open ocean supplies warmth and moisture that is 10‰ and 70‰ higher in $\delta^{18}O$ and δD, respectively, and 13‰ lower in *dxs*. Sea ice retreat also leads to other environmental changes, such as sea breeze development, that dramatically alter the nature of relationships between isotopes and many meteorological variables in summer. On shorter temporal scales, enhanced southerly flow promoted by negative NAO conditions produce higher $\delta^{18}O$ and δD values and lower *dxs* values. Diel isotopic cycles are generally very small as a result of a moderated coastal climate and counteracting isotopic effects of the sea breeze and local evaporation. Future losses in Baffin Bay sea ice extent will likely shift mean annual isotopic compositions toward more summer-like values, and past reductions should be similarly preserved in local glacial ice. These findings highlight the strong influence local environment has on isotope dynamics and the need for dedicated, multi-season monitoring to fully understand the controls on water vapor isotope variability.

https://doi.org/10.5194/acp-2020-340
Preprint. Discussion started: 18 May 2020


Atmospheric Chemistry and Physics Discussions

1. Introduction

The Arctic environment is rapidly entering a new state dominated by warmer air temperatures in all seasons, accompanied by dramatic sea ice loss, ecological changes, and ice sheet mass loss. Improving our knowledge of how the Arctic water cycle responds to regional warming and develops feedbacks within the changing climate is key to planning for a more resilient Arctic environment and economy (Meier et al., 2006; Vihma et al., 2016). While many modeling and satellite-based studies are examining this issue (NOAA, 2019a), ground-based observations are still critical to understanding the present-day hydrological cycle and tracking ongoing changes in local environments (e.g., Steen-Larsen et al., 2014; Bonne et al., 2015; Klein et al., 2015; Casado et al., 2018). Despite this need, the Arctic is data-sparse in terms of spatial coverage and temporal span of quality surface observations, and more environmental monitoring efforts are needed across the region (particularly at the highest latitudes) to better capture the hydroclimate processes and moisture transport across the Arctic domain.

The stable isotopes of water are well-established environmental tracers of the water cycle, reflecting both local weather conditions as well as moisture history and synoptic patterns (Craig, 1961; Dansgaard, 1964; Rozanski et al., 1993; Gat, 1996). Although less commonly studied than lower latitude regions, analyses across the Arctic have also shown that local observations of water isotopes can reveal important connections to wider atmospheric parameters such as teleconnections and storm patterns (e.g., Moorman et al., 1996; Welker et al., 2005; Theakstone, 2011; Bailey et al., 2015b; Puntsag et al., 2016; Putman et al., 2017). While our knowledge of isotope dynamics in the hydrosphere is largely based on studies of precipitation and surface waters (e.g., Dansgaard, 1964; Rozanski et al., 1993; Welker, 2000; Gurney and Lawrence, 2004), the development of field-deployable infrared laser spectrometers has fostered a number of recent studies focused on water vapor. With their ability to analyze water isotopes with high frequency (>1/min) in a continuous vapor flow, these spectrometers are well-suited to long-term monitoring studies (Bailey et al., 2015a). Several studies at land-based sites in the high latitudes have reported continuous water vapor isotopic observations for periods ranging from a single season to multiple years (Table S1), and their data sets are already proving highly useful in understanding hydroclimate dynamics.

These observational studies are critical to tracking and understanding the ongoing climate changes in high latitude regions, especially as the impacts of amplified polar warming on global weather patterns are hotly debated (Francis and Vavrus, 2012; Francis et al., 2018; Pithan et al., 2018; Nusbaumer et al., 2019; Cohen et al., 2020). Already, the published results from these polar water vapor isotope sites have highlighted the potential in tracking shifting moisture sources during extreme weather events (Bonne et al., 2015; Klein et al., 2015) as well as the importance of local geography in short-term isotopic variability (e.g., Kopec et al., 2014; Bréant et al., 2019). However, these sites reflect only a small portion of the vast and diverse polar environment, and fewer than half report data covering multiple years. More spatial coverage and longer periods of record are needed to fully harness water vapor isotope monitoring to resolve unanswered questions on polar hydroclimate processes and to accurately predict and detect future changes.

https://doi.org/10.5194/acp-2020-340
Preprint. Discussion started: 18 May 2020


Atmospheric Chemistry and Physics Discussions

Greenland is particularly important to our efforts to better understand past, current, and future climate, as its immense ice sheet has archived millennia of past climate changes (e.g., Steffensen et al., 2008) and environmental feedbacks from the increasing Greenland Ice Sheet loss reverberate globally (e.g., Box et al., 2012; Nghiem et al., 2012; Castro de la Guardia et al., 2015). The declining extent and duration of sea ice in its surrounding oceans are altering atmospheric moisture fluxes and transport across the Arctic (Gimeno et al., 2019; Nusbaumer et al., 2019), restructuring marine and terrestrial ecology (Bhatt et al., 2017; Laidre et al., 2020), and harming the health and welfare of native communities (Meier et al., 2006). Northwest Greenland in particular is one of the fastest warming regions on Earth with massive ice loss observed from glacial retreat and surface ablation (van As, 2011; Carr et al., 2013; Noël et al., 2019). Despite Greenland's importance, water vapor isotope monitoring has only been reported from four locations on the island (Steen-Larsen et al., 2013; Bonne et al., 2014; Kopec et al., 2014; Bailey et al., 2015a), and one record (Summit) has not had its data published.

We present here a new multi-year dataset from Thule Air Base in northwest Greenland that has recorded stable oxygen and hydrogen ratios ($\delta^{18}O$ and δD, respectively) of ambient water vapor nearly continuously from 04 August 2017 through 31 August 2019. As a result, this record is the first reported for Greenland that continuously spans over two years, critically giving a second set of observations to derive annual patterns and anomalies. Thule Air Base has been a focus of High Arctic research for many years (e.g., Schytt, 1955; Mastenbrook, 1968; Sullivan et al., 2008; Rogers et al., 2011; Leffler and Welker, 2013; Schaeffer et al., 2013), and our observing station on northern Baffin Bay allows a focus on how changing seasonal and interannual sea ice coverage affect the local climate and water vapor isotopes.

Our research addresses how interactions between the hydroclimate, cryosphere, and ocean are manifested in water vapor isotopes. The long period of record and very high frequency of isotopic (~1 observation per second, aggregated to 10 min) and meteorological observations (10 min) enable us to study water vapor isotope dynamics across varying temporal scales from diurnal to interannual. This Thule dataset and continuing observations at the base are part of the MOSAiC (Multidisciplinary drifting Observatory for the Study of Arctic Climate) project's Arctic Water Isotope Network (Welker et al., 2019; MOSAiC, 2020), a series of nine pan-Arctic sites simultaneously observing water vapor isotopes. To that end, our research at Thule provides a focused examination of the many local and regional environmental controls on water vapor isotopes at a coastal High Arctic site in northwest Greenland.

2. Field description

2.1 Local landscape

Our water vapor isotope observation station is located at Thule Air Base on the Pituffik Peninsula in far northwest Greenland (Fig. 1). Landmarks are referred to in this paper by their locally-known English names with Greenlandic names also listed when known. The main base and airfield, established in 1951 by the United States and Denmark, occupy a low-lying (< 100 m a.s.l.) region along the North River (Pitugfiup Kûgssua) facing North Star Bay and Bylot Sound, small arms of Baffin Bay

https://doi.org/10.5194/acp-2020-340
Preprint. Discussion started: 18 May 2020


Atmospheric Chemistry and Physics Discussions

semi-protected by Saunders and Wolstenholme Islands (Appat and Qeqertarsuaq). The main base is bracketed to the south and north by two broad ridges (300 and 240 m a.s.l., respectively) locally called South Mountain (Akínarssuaq) and North Mountain. Other military installations, both abandoned and presently occupied, are scattered throughout the wider Thule Defense Zone that covers the northern half of the peninsula. Near the southern edge of the Thule Defense Zone lies higher terrain including P-Mountain (Pingorssuit), the highest point of the Pituffik Peninsula at 815 m.

To the north, Wolstenholme Fjord (Uummannap Kangerlua) separates the Pituffik Peninsula from Steensby Land and the North Ice Cap (summit > 1200 m). The land-terminating margin of the Greenland Ice Sheet is approximately 14 km southeast of the main base and extends as low as 300 m a.s.l. This local section of the ice sheet, known as the Tuto Ice Dome, has a summit greater than 800 m a.s.l. and a mass balance that is semi-independent from the main Greenland Ice Sheet (Schytt, 1955; Hooke, 1970; Reeh et al., 1990). In addition, rugged terrain and mountains over 600 m a.s.l. run along the southern coastline of the peninsula toward Cape York.

2.2 Local climate

Thule has a polar desert/semi-desert climate (Gold and Bliss, 1995; Sullivan et al., 2008), with a mean annual temperature of -10.0°C and mean monthly temperatures ranging from -23.7°C in February to +6.5°C in July (2000–2018 observations, USAF, 2019). The high latitude (76° N) produces long periods of polar night (November–February) and midnight sun (May–August), and daylength changes by 15–30 minutes each day during transitional months. Extended periods of extremely cold temperatures below -25°C are frequent, and frosts and snowfall are possible in all months. Mean monthly temperatures are above freezing for only the three summer months, but summer can be surprisingly mild under continuous insolation with inland temperatures sometimes rising above 10°C. Coastal sea ice and the seasonal snow pack develop by October and last through May to early June (Barber et al., 2001; Fetterer et al., 2017; Stroeve and Meier, 2018; USAF, 2019). At early spring maximum, sea ice covers Baffin Bay over 1000 km south of Thule, except for the biologically important North Water Polynya located to the northwest (Barber et al., 2001; Tang et al., 2004; Heide-Jørgensen et al., 2016).

Annual precipitation is 130 mm water equivalent with half of this precipitation falling mostly as rain in June–August (USAF, 2019). Moisture in western Greenland primarily is sourced from the North Atlantic, but local sources of moisture, such as Baffin Bay, increase in importance during sea ice retreat in summer and early fall (Sodemann et al., 2008; Gimeno et al., 2019; Nusbaumer et al., 2019). Although the wind at Thule makes accurate snow measurements difficult and prone to overestimation (Chen et al., 1997), existing records report an average annual snowfall of 900 mm and October–December as the snowiest months (USAF, 2019). Synoptic storm systems dominate short-term weather variability with the dominant storm track consisting of extratropical cyclones that form to the south in Labrador Bay before tracking north and strengthening over Baffin Bay (Chen et al., 1997). These cyclones can be very intense, including a 333 kmh^{-1} observation in 1972 that is among the highest winds ever recorded on Earth (Stansfield, 1972; Moore, 2016). Atmospheric rivers (narrow corridors of strong horizontal moisture advection) have outsized effects on polar weather (Woods et al., 2013; Liu and Barnes, 2015; Wille et al.,

https://doi.org/10.5194/acp-2020-340
Preprint. Discussion started: 18 May 2020


Atmospheric Chemistry and Physics Discussions

125 2019), and periods of intense ice sheet melt and mass loss in Greenland, such as July 2012, often coincide with atmospheric rivers affecting the ice sheet (Neff et al., 2014; Bonne et al., 2015; Mattingly et al., 2018; Ballinger et al., 2019; Oltmanns et al., 2019).

Differential radiative heat loss between the ice sheet and coastal region drives katabatic winds (van As et al., 2014) from the east and southeast that dominate the wind regime in Thule outside of the summer months. From April through September, a 130 west to northwest sea breeze develops along the coast due to differential warming between the ocean and the local area of snow-free tundra (Atkinson, 1981), and it brings cooler marine surface air, often associated with fog, several kilometers inland. This sea breeze generally strengthens in the afternoon and weakens at night, though continuous summer insolation often prevents a full shift to nightly katabatic flow as observed at other sites (e.g., Kopec et al., 2014). These two wind patterns at Thule produce an overall bimodal wind distribution with azimuth peaks at 100° (katabatic) and 270° (sea breeze).

135 ## 3. Methods

3.1 Equipment setting

A Picarro L2130-i with Standards Delivery Module (SDM) setup was installed in a temperature-controlled building on the crest of South Mountain (76.514° N 68.744° W, 229 m a.s.l.) in October 2016, with quality data observations beginning in August 2017 after a system reset. The L2130-i + SDM uses cavity ring-down spectroscopy to measure $\delta^{18}O$ and δD in ambient 140 water vapor and is particularly amenable to long-term monitoring with limited human interaction. Tygon tubing (3/4 in) connects the L2130-i to the collection point on the roof of the building, away from parking and idling zones as well as building exhaust. The building is heated and always warmer than ambient outside air, even during extreme warm events in summer, which limits potential condensation within the tubing.

Local air flow is unimpeded by topographic barriers from any direction within 20 km. When the summer sea breeze drives a 145 shallow marine air mass inland, the resulting inversion boundary and associated fog often overtops the South Mountain ridge and reaches the L2130-i's intake. Potential anthropogenic impacts to observations at the monitoring site are limited as the main base lies 2 km to the north and 200 m lower in elevation. Typically, less than 20 vehicles a day travel the access road that is 200 m from the building housing the L2130-i, and visitors are uncommon.

3.2 Isotopic observations and calibrations

150 Our L2130-i at Thule takes an observation of ambient water vapor $\delta^{18}O$ and δD approximately once per second, and deuterium-excess values (*dxs*) are calculated from each isotope observation by $dxs = \delta D - 8 * \delta^{18}O$ (Dansgaard, 1964). Observations were continuous from August 2017 through August 2019 except for one period when the analyzer suffered power failure (05–13

https://doi.org/10.5194/acp-2020-340
Preprint. Discussion started: 18 May 2020


Atmospheric Chemistry and Physics Discussions

Sep 2018). Some additional gaps in the data were introduced as a result of quality checking (S1) and standard calibrations, but these gaps were typically less than 24 hours in duration.

Calibrations were performed through the SDM every 25 hours by injecting two water standards, USGS 45 ($\delta^{18}O$ = -2.24‰, δD = -10.3‰) and USGS 46 ($\delta^{18}O$ = -29.80‰, δD = -235.8‰), sequentially into a stream of air supplied by a dry air canister for standardization to the SMOW-SLAP scale. Each standard was injected for 10 minutes, as repeated tests at Thule showed this to be the minimum time needed to reach stable isotopic value readings. This calibration interval and duration is longer and shorter, respectively, than in other similar studies (e.g., Bastrikov et al., 2014; Bailey et al., 2015a; Bréant et al., 2019), but deemed a necessary balance to extend the life of the dry air canister and standard waters at the remote location while still allowing an estimate of the machine's accuracy drift. The mean of the last 200 seconds of each standard injection was kept as the final isotopic value for each standard calibration.

This calibration dry air system was installed in August 2019; before, standards were injected into an air stream dried by a Drierite column. However, the Drierite column does not fully remove all ambient moisture and increasingly lost effectiveness over time at Thule. The residual ambient moisture had a significant effect on observed isotopic values during calibrations, and very few of the calibration runs prior to the dry air installation accurately recorded the standard values needed to correct for machine analytical drift. These residual ambient moisture effects were eliminated after the dry air installation.

Due to the poor calibration quality for most of our observation period, we did not apply a daily drift correction to the isotopic data. Forty-three calibrations completed after the dry air installation show consistently high precision and limited day to day sensor drift (Table S3). The average standard error for a calibration of 200 individual observations was ±0.04‰ and ±0.3‰ for $\delta^{18}O$ and δD, respectively, with the same error magnitude for both standard waters. The standard deviations (σ) of the 43 calibration means for $\delta^{18}O$ and δD were 0.2‰ and 0.6‰, respectively, with deviations the same for both standard waters. The maximum difference between any two calibration run means were 1.0‰ and 2.7‰ for $\delta^{18}O$ and δD, respectively. Thus, while calibration uncertainties are not calculated over our entire record, natural short-term isotopic variability and large seasonal patterns are unlikely to be severely affected by the relatively small measurement uncertainty due to analytical drift (e.g., Steen-Larsen et al., 2013; Bréant et al., 2019).

At lower water vapor mixing ratios (<1500 ppmv), the L2130-i loses accuracy and precision, and a humidity response curve must be developed in order to correct for any analytical bias in isotopic values (Steen-Larsen et al., 2013; Bastrikov et al., 2014; Bailey et al., 2015a). In July 2019, the two standard waters were each injected for 10 minutes at ten different flow rates to produce a sequence of standard observations between 500 and 7000 ppmv. Humidity response curves were created using nonlinear regression to correct ambient observations for sensor biases at low humidity (S2, Fig. S1). For $\delta^{18}O$, the 95% confidence intervals for humidity response corrections range from ±0.24‰ at 500 ppmv to ±0.09‰ for all observations higher than 1500 ppmv, and for δD, the 95% confidence intervals range from ±1.6‰ at 500 ppmv to ±0.6‰ for all observations higher than 1500 ppmv. Additionally, our machine has a consistent accuracy offset of +1.92‰ and +1.13‰ respectively in all

https://doi.org/10.5194/acp-2020-340
Preprint. Discussion started: 18 May 2020


Atmospheric Chemistry and Physics Discussions

185 $\delta^{18}O$ and δD observations with mixing ratios higher than 1500 ppmv. However, our humidity response correction incorporates and corrects this offset.

Ambient observations with a mixing ratio less than 500 ppmv fell outside our humidity response observations and were thus excluded from further analysis (fewer than 500 individual 1 s observations). After the humidity response corrections, data were quality checked and offending data (e.g., extreme outliers, residual calibration vapor impacts, extreme moisture spikes 190 unrelated to weather) removed. The quality checked isotope data were aggregated into 10 min, 1 h, and daily means.

3.3 Meteorological observations

An automated weather station (SMT, for South Mountain), located on the roof of the building that houses the L2130-I, took a reading of air temperature, relative humidity (with respect to the saturation vapor pressure over ice), and station barometric pressure every 10 minutes throughout the duration of isotopic observations (Muscari, 2018). For analysis at different temporal 195 resolutions, these data were also aggregated into 1 h and daily means. The L2130-i takes a reading of the water vapor mixing ratio with every isotopic observation, and observations of this variable were aggregated to 10 min, hourly, and daily means and added to the SMT datasets.

Hourly mean near-surface wind speeds and azimuths (USAF, 2019) were taken at the Thule Airport (THU), aggregated to daily values, and joined to the hourly and daily SMT databases. While the THU recording station is 170 m lower than SMT, 200 the two stations are less than 1 km apart and their meteorological data agree well ($\rho_{temperature} = 0.98$, $\rho_{dew.point} = 0.98$, $\rho_{station.pressure} = 0.96$). Daily climate teleconnection indices for the North Atlantic Oscillation (NAO) and Arctic Oscillation (AO) were downloaded from the US National Weather Service Climate Prediction Center (NOAA, 2019b) and joined with the daily SMT database. Daily sea ice extent for Baffin Bay was obtained through the National Snow and Ice Data Center (NSIDC) Multisensor Analyzed Sea Ice Extent (MASIE) product (Fetterer et al., 2010).

205 To reduce issues with the radial nature of azimuth data during correlation analysis, wind azimuths were converted to 'katabatic deviations' where an azimuth of 100° (i.e., the mean katabatic wind azimuth) was defined as zero, and other observations were redefined as their minimum absolute degree distance from 100°. The katabatic deviations therefore range in value between 0° and 180°, and while this does not fully solve the radial issue (e.g., a katabatic deviation of 80° can represent both a northly 20° wind or a southerly 180° wind), it fares well in distinguishing between the bimodal "southeasterly katabatic" and 210 "northwesterly sea breeze" regimes.

3.4 Statistical analyses

Spearman correlations between isotopic and meteorological variables were calculated across the full datasets at all three temporal resolutions. Strong correlations that arise between variables in this analysis, though, may be spurious due to common responses to seasonal change. Likewise, variables that do not have a seasonal cycle, such as relative humidity, may have

https://doi.org/10.5194/acp-2020-340
Preprint. Discussion started: 18 May 2020


Atmospheric Chemistry and Physics Discussions

stronger correlations once the interference from seasonality is removed. To examine this, we removed the strong seasonal cycles of the isotopic values, air temperature, and mixing ratio by sinusoidal curves fitted to the annual cycle of each full data time series. With these seasonally-adjusted data, we calculated a second set of correlations.

Data at each temporal resolution were also binned by month, and correlations then calculated for each month to examine seasonal changes in isotope-climate relationships. To assess temporal covariance and possible lead/lag relationships between teleconnection indices (NAO, AO) and isotopic variables, we performed cross-correlation analysis (Addinsoft, 2020) with a first differencing methodology (Peterson et al., 1998) to remove autocorrelations and avoid cross-correlation bias (Olden and Neff, 2001; Runge et al., 2014).

3.5 Back-trajectory analysis

We compiled a Thule-specific moisture sourcing and transportation "quasi-climatology" with air parcel back-trajectory analysis using the HYSPLIT trajectory model forced with MERRA-2 reanalysis data (Stein et al., 2015; Gelaro et al., 2017). To build this "quasi-climatology", we randomly selected 10 days from each month during 1980–2018 as we judged 10 days to provide a robust representation of the true climatology while remaining within reasonable computation and data storage limits. We then initiated 10-day back trajectories for each day from the MERRA-2 grid point nearest Thule at the four synoptic hours (0000, 0600, 1200, and 1800 UTC) on 6 vertical levels (10, 100, 200, 500, 1000, and 1500 meters above ground level), resulting in 2880 total trajectories. Following previous studies (e.g., Sodemann et al., 2008; Molina and Allen, 2019), the moisture uptake algorithm implemented in the PySPLIT python library (Warner, 2018) infers moisture uptake into the parcel when changes in specific humidity (Δq) > 0.2 g kg^{-1} and precipitation when Δq < -0.2 g kg^{-1}. Later moisture uptakes are weighted more heavily than uptakes occurring prior to precipitation (Sodemann et al., 2008). A domain covering Baffin Bay from the Davis Strait to Nares Strait was defined, and the percentage of moisture uptake occurring within and outside this domain was calculated with raw values at each grid cell multiplied by the cosine of latitude to compensate for smaller grid cell area with northward extent.

4. General overview of isotopic results

The mean annual $\delta^{18}O$ and δD values at Thule are -33.0 ± 5.9‰ and -248 ± 41‰, respectively (10 min data, mean ± 1 σ). Over the full dataset, $\delta^{18}O$ and δD have a strong linear relationship with low parameter standard error: $\delta D = 6.959 \pm 0.003 * \delta^{18}O - 18.07 \pm 0.09$‰ ($r^2 = 0.98$, n=111138, 10 min data). Overall, this value is comparable to other slopes observed at other high latitude sites, such as 6.8 at Ivittuut, Greenland, (Bonne et al., 2014), 6.5 at NEEM, Greenland, (Steen-Larsen et al., 2013), 6.0–6.5 at Dome C, Antarctica (Casado et al., 2016), and 6.95 from the vapor mixing line at Kangerlussuaq, Greenland (Kopec et al., 2014). Changes in $\delta^{18}O$ are thus closely mirrored in δD, and most differences are only detectable on very short timescales (i.e., less than hourly) when some minor lead-lag between relative maxima and minima may occur.

https://doi.org/10.5194/acp-2020-340
Preprint. Discussion started: 18 May 2020


Atmospheric Chemistry and Physics Discussions

The *dxs* at Thule is negatively correlated with both $\delta^{18}O$ and δD (ρ_{10min} = -0.76 and -0.67, respectively). Temporal aggregation reduces the overall range and variability of isotopic data by reducing extreme values, but this does not greatly affect the distribution or means. Generally, conclusions drawn from one level of aggregation are consistent across all levels of aggregation, and no exceptional cases were identified in this study.

The isotopic records show a strong annual cycle, with the highest values for $\delta^{18}O$ and δD in summer and lowest values in winter and early spring, while *dxs* values have the opposite pattern with minimum values in summer and maximum values in winter (Fig. 2, Table 1). The isotopic values also have very wide overall ranges, with $\delta^{18}O$, δD, and *dxs* spanning over 30‰ (-49.5‰ to -17.5‰) 230‰ (-377‰ to -142‰), and 55‰ (-7.6‰ to 47.5‰) respectively, in our 10-minute database. Although diel cycles in isotopes are very small (generally <1‰ for $\delta^{18}O$ and *dxs*), the magnitude of irregular hourly to weekly variations in isotopic values can approach 30–50% of the entire annual range.

Among meteorological variables, mixing ratio has the strongest correlation to all isotopic species ($\rho_{\delta18O.10min}$ = +0.83, $\rho_{\delta D.10min}$ = +0.79, $\rho_{dxs.10min}$ = -0.79) followed closely by air temperature ($\rho_{\delta18O.10min}$ = +0.76, $\rho_{\delta D.10min}$ = +0.72, $\rho_{dxs.10min}$ = -0.74). Katabatic deviation (i.e., wind direction) ($\rho_{\delta18O.hr}$ = +0.49, $\rho_{\delta D.hr}$ = +0.46, $\rho_{dxs.hr}$ = -0.50) and the NAO ($\rho_{\delta18O.day}$ = -0.17, $\rho_{\delta D.day}$ = -0.14, $\rho_{dxs.day}$ = +0.22) have moderate correlation strengths, while other variables have limited correlation strength. Temporal aggregation slightly strengthens correlations (likely due to reduced impact of extreme values), but does not generally change the order of variables when ranking by correlation strength (i.e., mixing ratio always has the strongest correlation, followed by air temperature). Seasonally-adjusting the data weakens nearly all correlations by removing the common response to seasonal change, but strengthens isotopic correlations with relative humidity ($\rho_{\delta18O.10min}$ = +0.33, $\rho_{\delta D.10min}$ = +0.33, $\rho_{dxs.10min}$ = -0.24). Cross-correlation analysis found statistically significant correlations between the NAO and meteorological variables (air temperature, mixing ratio, station pressure) at Thule with zero-day lag, with $\delta^{18}O$ and δD at a three-day lag, and with *dxs* at a two-day lag.

5. Environmental controls on water vapor isotopes at Thule

Based on our statistical analyses and personal field observations, the values of water vapor isotope ratios at Thule are determined largely by five interacting factors: a) local air temperature, b) local marine moisture availability, c) synoptic moisture transport, d) surface wind regimes, and e) the evaporation/sublimation of local surface waters and snow. These factors interact and compete with each other, with the dominance of particular factors varying over the course of a year with the changing seasons. To clarify this complex situation, this discussion will first detail the effects of the these factors as expressed specifically in the Thule environment. The impact of these factors on isotopic systematics will then be examined at annual, synoptic, and diel cycles to reveal how observed isotopic values are produced.

https://doi.org/10.5194/acp-2020-340
Preprint. Discussion started: 18 May 2020


Atmospheric Chemistry and Physics Discussions

5.1 Air temperature

Our back-trajectory analysis shows that most water vapor is supplied to Thule from evaporation in more southerly locations and then advected north along the western coast, with a substantial fraction of this water vapor having previously passed over the southern Greenland Ice Sheet (Fig. 3a). As the air mass cools in this northerly transport, water vapor will condense into precipitation that selectively removes isotopically heavier water molecules (Dansgaard, 1964; Rozanski et al., 1993). This Rayleigh fractionation results in an air mass with water vapor that is increasingly isotopically lighter (i.e., depleted in ^{18}O and ^{2}H) as it travels to Thule, and colder conditions at Thule create a steeper temperature gradient with the more southerly moisture source that enhances the degree of fractionation (e.g., Rozanski et al., 1993; Bonne et al., 2014; Kopec et al., 2019). This connection is manifested in our strong correlations of $\delta^{18}O$ and δD with air temperature ($\rho_{\delta 18O.10min} = +0.76$, $\rho_{\delta D.10min} = +0.72$), which are surpassed in strength only by correlations with the closely linked mixing ratio.

However, strong annual correlations between water isotopes and temperature are increasingly shown to result from common responses between air temperature and other variables that also follow seasonal patterns (e.g., Akers et al., 2017). This also appears true for Thule, as the correlations are much weaker when seasonal cycles are removed ($\rho_{SA\text{-}\delta 18O.10min} = +0.32$, $\rho_{SA\text{-}\delta D.10min} = +0.24$). Most likely, much of the strength of the non-seasonally adjusted correlations is due to the common response with broader environmental changes linked to seasonally-covarying sea ice extent. Despite this, the weaker seasonally-adjusted correlations show that a temperature effect is still expressed to a weaker degree in shorter-term, intra-seasonal isotopic variations.

Temperature-driven equilibrium fractionation has a much more limited impact on *dxs* values than $\delta^{18}O$ and δD values (Pfahl and Sodemann, 2014; Dütsch et al., 2017). However, *dxs* values at Thule have a strong correlation with air temperature ($\rho_{dxs.10min} = -0.79$), and the correlation using seasonally adjusted data is actually much stronger ($\rho_{SA\text{-}dxs.10min} = -0.49$) than those observed in $\delta^{18}O$ and δD. Temperature-driven changes on *dxs* have been reported (Jouzel and Merlivat, 1984; Dütsch et al., 2017; Kopec et al., 2019), particularly for very cold conditions, and it is possible that this is contributing to the short-term correlation between *dxs* and both $\delta^{18}O$ and δD as well as the strong correlations between *dxs* and air temperature. However, it is more likely that the *dxs* changes that are driving these strong short-term correlations with temperature are, like with $\delta^{18}O$ and δD, actually responding to another environmental factor that covaries with temperature, like surface wind regime.

5.2 Local marine moisture availability

The isotopic composition of water vapor in an air mass is initially determined by environmental conditions at the original site of vapor uptake, such as the ocean surface. As a result, moisture sources with different environments can imprint identifiable isotopic compositions to water vapor that are then preserved through later transport (e.g., Pfahl and Sodemann, 2014; Bonne et al., 2015; Dütsch et al., 2017; Bonne et al., 2019). Changes in the *dxs* of ice cores, precipitation, and water vapor has been used to reconstruct moisture source changes across seasons as well as extending back deep through time (e.g., Steffensen et

https://doi.org/10.5194/acp-2020-340
Preprint. Discussion started: 18 May 2020


Atmospheric Chemistry and Physics Discussions

al., 2008; Feng et al., 2009; Steen-Larsen et al., 2013; Osterberg et al., 2015). At Thule, seasonal sea ice changes permit or restrict the delivery of local moisture from the nearby ocean, and this availability is a primary control on mean isotopic values.

Our back-trajectory analysis shows that the regions of predominate water vapor uptake for air masses arriving at Thule vary substantially over the year (Fig. 3b). Baffin Bay is the dominant evaporative moisture source from the late spring through early winter, contributing ~50% of water vapor transported to Thule (Table S4). Substantial contributions from the Labrador Sea, Denmark Strait, Hudson Bay, and Canadian Arctic Archipelago regions are also observed during this time. These local polar waters have high surface relative humidity when open in summer (Fig. 3c) and supply Thule with water vapor that has high $\delta^{18}O$ and δD values and low *dxs* values.

From January until May, local seas are extensively ice covered and the majority of water vapor present at Thule originates from more distant sources in the Labrador Sea and North Atlantic (Fig. 3b). Large evaporation events in the North Atlantic tend to occur in the cold sector of extratropical cycles (Aemisegger, 2018; Aemisegger and Papritz, 2018) where the dry air (Fig. 3c) produces water vapor with high *dxs* values. As this moisture travels north to Thule, fractionation from rain out during transport results in isotopically light water vapor, and sea ice coverage in Baffin Bay and other local Thule waters prevent isotopic exchange that would mitigate some of this fractionation. Interestingly, our analysis reveals a large amount (>30%) of Thule's winter water vapor is supplied by sections of southern Baffin Bay and the Labrador Sea with 5–95% climatological mean sea ice cover. As surface relative humidity is very low above forming sea ice, any vapor picked up in these regions will have exceptionally high *dxs* values and enhance the high *dxs* values coming from the distant winter sources (Kurita, 2011).

5.3 The NAO and synoptic moisture transport

Phase changes in the NAO can serve to enhance or limit moisture transport from the south to Thule (Fig. 3a) as atmospheric mass is redistributed between the Arctic and North Atlantic and synoptic flow patterns near Greenland are affected. Changes in water isotopes that result from these atmospheric shifts have been detected in Arctic snow (e.g., Vinther et al., 2003) and plants (Welker et al., 2005). However, the strength and nature of the relationship is not consistent across Greenland (Zheng et al., 2018) due to different spatial responses in moisture transport (Vinther et al., 2010; Bjørk et al., 2018).

In western Greenland, the negative phase of the NAO (NAO-) is associated with enhanced southerly flow that brings warmer temperatures and greater regional snow, while the positive phase (NAO+) has stronger westerlies that limit the northward penetration of southern air masses (Sodemann et al., 2008; Bjørk et al., 2018). These effects are manifested in our observations where more negative NAO indices are correlated with a stronger Greenland anticyclone (i.e., higher Thule station pressure, $\rho_{NAO.pres} = -0.59$). When southerly advection along the western edge of the anticyclone is promoted during NAO- phases, Thule tends to be warmer ($\rho_{NAO.SA\text{-}temp} = -0.29$) and have a higher mixing ratio ($\rho_{NAO.SA\text{-}MR} = -0.27$). We did not find noteworthy correlations with the AO at Thule, likely because changes in AO phase relate to pan-Arctic conditions while the NAO changes are more focused on Greenland and the North Atlantic.

https://doi.org/10.5194/acp-2020-340
Preprint. Discussion started: 18 May 2020


Atmospheric Chemistry and Physics Discussions

Cross-correlation analysis (Fig. 4, Fig. S2) reveals that shifts to more negative NAO indices produce isotopically heavier water vapor observations with lower *dxs* values two to three days later at Thule, presumably as air advected north over Baffin Bay picks up local moisture and/or the warmer conditions reduce the degree of fractionation during transport. Although the differencing required for cross-correlation analysis produces weaker correlations than those calculated with seasonally-adjusted data, both correlation analyses agree that NAO- conditions are warmer and wetter at Thule.

The relationship between water vapor isotopes and NAO phases across interannual timeframes at Thule is unclear from our data's limited period of record, but climatology and ice core studies show clear impacts on Greenland's precipitation, glacial mass balance, and sea ice at this scale (Stern and Heide-Jørgensen, 2003; Vinther et al., 2003; Sodemann et al., 2008; Bjørk et al., 2018). NAO indices in summer 2018 were almost continuously positive, coinciding with relatively cool conditions at Thule and below average melt of the northwestern Greenland Ice Sheet. In contrast, summer 2019 was dominated by NAO- conditions, was nearly 4°C warmer than 2018 at Thule, and Greenland saw near-record ice sheet melt (Maslanik and Stroeve, 1999; USAF, 2019). Despite these dramatically different conditions, mean $\delta^{18}O$ and δD values are practically identical between the two summers (<0.01‰ and <1‰ different, respectively) and mean *dxs* values differ only by 1‰. This suggests that changes in synoptic flow patterns have little impact when local seas are free of sea ice, as isotopic exchange with local marine moisture can buffer any potential isotopic changes from longer-distance synoptic transport shifts.

However, spring 2018 was also characterized by NAO+ indices and colder conditions while spring 2019 had lower NAO indices and warmer weather. In contrast to the summer observations, $\delta^{18}O$ and δD values are 4.4‰ and 34‰ higher, respectively, in spring 2019 than spring 2018, and *dxs* values are 1.7‰ lower. As sea ice is still largely intact through spring near Thule, the limited potential for local water input and exchange at this time appears to allow an NAO signal to be expressed in the mean isotopic values. Additional seasons and years of observation with different NAO conditions will help clarify the magnitude and seasonal extent of interannual effects from the NAO on Thule water vapor isotopes.

5.4 Surface wind regimes

Between April and September, the surface winds at Thule alternate between southeasterly katabatic winds off the nearby ice sheet and a northwesterly sea breeze from Bylot Sound, although not necessarily on a regular daily cycle. Such wind shifts at other coastal sites are isotopically identifiable because katabatic winds source isotopically light vapor from ice sheets while sea breezes source isotopically heavy vapor from the nearby ocean (e.g., Kopec et al., 2014; Bréant et al., 2019). After adjusting for the seasonal biases at Thule where katabatic winds dominate in colder months and the sea breeze dominates in warmer months, a weak correlation between katabatic deviation (i.e., sea breeze occurrence) and the water vapor isotopes ($\rho_{\delta 18O.hr}$ = +0.20, $\rho_{dxs.hr}$ = -0.21) suggests that on a given day the sea breeze will bring isotopically heavier water vapor with lower *dxs* values than katabatic flow. This is supported by personal field observations on multiple occasions in summer 2018 and 2019

https://doi.org/10.5194/acp-2020-340
Preprint. Discussion started: 18 May 2020


Atmospheric Chemistry and Physics Discussions

when a shift to a sea breeze brought notably cooler and more humid conditions along with a real-time rise in $\delta^{18}O$ and δD on the L2130-i.

However, although the difference in mean isotopic values are statistically significant for all isotopic species ($p < 0.001$, Welch's t-test) between the two wind regimes, there is substantial overlap in the overall range (May–September data, mean ± σ: $\delta^{18}O_{sea.breeze}$ = -26.8±3.5‰ vs. $\delta^{18}O_{katabatic}$ = -28.5±3.1‰, $\delta D_{sea.breeze}$ = -207±25‰ vs. $\delta D_{katabatic}$ = -219±22‰, $dxs_{sea.breeze}$ = 7.6±4.8‰ vs. $dxs_{katabatic}$ = 9.3±4.8‰, Fig. S3). The isotopic difference between the two wind regimes may be smaller at Thule than other studied sites because of Thule's location on the west-pointing Pituffik Peninsula. Much of the southeasterly katabatic flow here is not sourcing air directly off the main Greenland Ice sheet, but rather air that is traveling over Baffin Bay along the western coast and potentially even over nearby De Dødes Fjord (Fig. 1). Thus, both the katabatic winds and the sea breeze are bringing water vapor from locations where it has been able to isotopically exchange with local ocean waters.

The slightly lower water vapor isotope values during katabatic flow is then likely due to the vapor's brief passage over topographic highs of Cape York and the Tuto Ice Dome while the sea breeze carries moisture onshore unimpeded from Bylot Sound. Additionally, we note that as our wind data comes from a lower elevation site than our isotopic sampling, it is possible that particularly shallow sea breezes could produce wind observations identified as 'sea breeze' while the air on South Mountain is still katabatic sourced. However, no consistently clear signs of different air masses affecting the two stations in summer were found when examining periods with anomalous observations (e.g., sea breeze azimuth with high air temperature).

5.5 Evaposublimation of local snow and surface waters

Evaporation and sublimation of local surface waters and snowpack (referred here as "evaposublimation") can also alter local water vapor isotopic values by supplying vapor that is isotopically light with higher *dxs* values relative to the snow/ice/water's isotopic composition, (Casado et al., 2018; Kopec et al., 2019). Most of the snow at Thule falls in autumn and early winter (USAF, 2019) and surface waters in Thule generally match the isotopic composition of the winter snowpack (Csank et al., 2019). Thus, evaposublimation during warmer months will generally serve to lower $\delta^{18}O$ and δD values and raise *dxs* values of water vapor in the local environment. Additionally, very warm events in summer induce surface melt and sublimation across the Tuto Ice Dome and Greenland Ice Sheet (Box and Steffen, 2001; Nghiem et al., 2012; van As et al., 2012; Neff et al., 2014). Any of this moisture reaching Thule would be depleted in ^{18}O and ^{2}H and have a higher *dxs* relative to typical summer ocean-sourced moisture as it originates in a higher and colder location on the ice sheet. Isotopic effects from plant transpiration (Gat and Matsui, 1991; Farquhar et al., 2007; Aemisegger et al., 2014) are not expected to be of much impact due to the sparse plant cover at Thule (Gold and Bliss, 1995).

https://doi.org/10.5194/acp-2020-340
Preprint. Discussion started: 18 May 2020


Atmospheric Chemistry and Physics Discussions

5.6 Summary of environmental drivers of water vapor isotopes at Thule

To summarize, observations at Thule when the water vapor $\delta^{18}O$ and δD values are higher and *dxs* values are lower could be a result of: a) warmer local air temperature, b) more local marine moisture source, c) synoptic pattern that favors more southern flow (i.e., NAO-), d) sea breeze surface winds, and/or e) lower evaposublimation. Likewise, lower $\delta^{18}O$ and δD values and higher *dxs* values are due to: a) colder local air temperature, b) more distant marine moisture source, c) synoptic pattern that restricts southern flow (i.e., NAO+), d) katabatic surface winds, and/or e) higher evaposublimation. These different factors operate on different temporal scales (Fig. 5a). For example, shifts in local versus distant moisture sourcing affect isotopic composition at all scales, but evaposublimation is mostly important only on shorter timescales like diel cycles.

Additionally, these factors interact greatly with each other, and isotopic variability cannot and should not be reduced down to a single predominant driver. However, these factors largely interact constructively to enhance relationships between environmental conditions and water vapor isotopic values (Fig. 5b, c). For example, the NAO- enhances southerly advection to Thule, which results in warmer local air temperature and potentially reduced sea ice extent that exposes local waters. Similarly, the sea breeze is enhanced during warmer periods of the year when sea ice extent is low, and it directly supplies local moisture to Thule from Bylot Sound. All these factors support isotopically heavier water vapor isotopes with lower *dxs* values.

The main exception to these constructive interactions is evaposublimation, which supplies isotopically light vapor with high *dxs* during warmer periods which would otherwise favor higher $\delta^{18}O$ and $\delta^{2}H$ values and lower *dxs* values as previously described. Due to the ample supply of marine moisture in the coastal Thule setting, evaposublimation is not expected to be a predominant moisture source or primary driver of isotopic variability. However, periods where water vapor isotopes are lighter and *dxs* values higher than expected for a given temperature may be a good identifier of an evaposublimation effect, and such analysis could be used to better quantify ice sheet vapor flux during large melt events.

6. Annual isotopic cycle

The strong annual cycle in water vapor isotopes at Thule (Fig. 2) is directly tied to seasonal changes in weather and the regional environment driven by the presence or absence of local sea ice. While the annual sea ice breakup directly influences vapor isotopic composition by allowing local marine moisture supply, it also produces a cascade of other environmental changes that also isotopically change water vapor at Thule (Fig. 5). Beyond simply affecting the mean values of water vapor isotopes, the dramatic environmental changes that occur at Thule after sea ice breakup also alter correlative relationships between isotopic and meteorological variables (Fig. 6). As a result of all these factors, the seasonal growth and breakup of the Baffin Bay sea ice is readily identifiable in our water vapor isotope record, particularly in the *dxs* data.

https://doi.org/10.5194/acp-2020-340
Preprint. Discussion started: 18 May 2020


Atmospheric Chemistry and Physics Discussions

6.1 Winter

During winter polar night when Baffin Bay is largely frozen over, the water vapor isotopic system at Thule is relatively simple. Mean values for winter $\delta^{18}O$ and $\delta^{2}H$ are lower and *dxs* values higher in the absence of a local marine moisture supply (Fig. 3b), and isotopic variability largely reflects extratropical cyclone impacts and broader synoptic flow. Strong winter correlations between isotopic species and both air temperature and mixing ratio (Fig. 6) reflect this as warmer and moister air transported to Thule produces higher water vapor $\delta^{18}O$ and δD values and lower *dxs* values.

The *dxs* values in winter are also notably more variable than during summer. Since nearly all moisture arriving to Thule in summer has to pass over the open water of Baffin Bay, vapor exchange and uptake probably helps stabilize the summer *dxs* variability. In contrast, when Baffin Bay is frozen, the *dxs* values from different moisture sources may be preserved better and contribute to the higher winter variability in *dxs* values. More focused back trajectory analysis on winter *dxs* variability in the future may help quantify the variability and effects of different moisture sources.

6.2 Spring and sea ice breakup

In both spring seasons covered by our record, the isotopic and meteorological variables have a very abrupt shift (beginning on 14 May 2018 and 29 Apr 2019) from winter-typical values to summer-typical values. During these shifts, temperatures rise more than 15°C in a few hours, followed by a 10‰ increase in $\delta^{18}O$ and 10–15‰ drop in *dxs* over the next few days. Sea ice concentrations and satellite imagery from NSIDC (Fetterer et al., 2017) and MODIS (Hall and Riggs, 2015) show that these abrupt spring shifts are associated with the breakup of sea ice near and to the northwest of Thule as well as a general reduction in sea ice concentration throughout Baffin Bay (Fig. S4). Similar isotopic responses to sea ice breakup have been previously reported in the Arctic Ocean as well (Klein and Welker, 2016). Before the breakups in 2018 and 2019, the NAO index drops 2 and 4 points, respectively, and the following extreme isotopic shifts creates very strong correlations in May between isotopic variables and both Baffin Bay sea ice extent (Fig. 6e) and the NAO index (Fig. 6f).

Sea ice breakup and environmental warming is followed in short order by the first sustained sea breeze developments of the year, also aiding the delivery of newly available local vapor to Thule. At this time in late spring, radiative heat loss at night drives a semi-consistent diel wind cycle between afternoon sea breezes and nightly katabatic flow. The environmental contrast between the relatively warm open ocean and still frigid Greenland Ice Sheet and tundra serve to maximize isotopic differences in the two wind regimes, with the strongest correlations between isotopic variables and katabatic deviation observed in April through June (Fig. 6d).

6.3 Summer

The height of summer brings dramatic changes in isotope-climate relationships. Correlation strength between isotopes and katabatic deviation collapses in midsummer, likely due to the increased dominance of the sea breeze that suppresses overall

https://doi.org/10.5194/acp-2020-340
Preprint. Discussion started: 18 May 2020


Atmospheric Chemistry and Physics Discussions

variability and buffers the local air mass against major isotopic changes with ample local marine moisture supply. Additionally, summer warming of tundra and the Greenland Ice Sheet reduces the environmental gradient with the open ocean, and the complete loss of fast ice in De Dødes Fjord and Melville Bay to the southeast of Thule allows katabatic flow to also source local waters.

More notably, the $\delta^{18}O$ and δD correlations with air temperature switch from positive to negative in summer months (mean $\rho_{non\text{-}summer}$ = +0.38 vs. mean ρ_{summer} = -0.32 for $\delta^{18}O$) with *dxs* showing a similar, though opposite, pattern (mean $\rho_{non\text{-}summer}$ = -0.53 vs. mean ρ_{summer} = +0.40 for $\delta^{18}O$) (Fig. 6a). As a result, the highest $\delta^{18}O$ and δD and lowest *dxs* values are not observed when air temperatures are greatest, but rather near 0°C (Fig. S3a, S3c) During the same summer period, isotopic correlations with mixing ratio greatly weaken (Fig. 6b) while correlations with relative humidity strengthen (Fig. 6c). The relationship between air temperature and mixing ratio, strongly correlated with a positive slope through most of the year, decouples in summer, and temperatures warmer than 5°C largely result in no higher water vapor content (Fig. S5)

Summer in Thule is relatively cool and humid under shallow marine air from local open seas, helped onto land by the sea breeze. As the local ocean never warms much above freezing, most of the warmest periods at Thule (i.e., >5–8°C) require a high pressure ridge over Greenland, often associated with southerly air flow up along the western Greenland coast and aided by NAO- conditions. In many cases, the position of this high favors large-scale downsloping and subsidence off the northwestern ice sheet (Fig. 7). This pattern was exceptionally persistent in summer 2019 (Tedesco and Fettweis, 2019), and most of our very warm observations at Thule com during this period. Moisture arriving at Thule through southerly advection and/or downsloping in these warm events is isotopically lighter and less humid than local marine air as it is more distantly sourced and also must cross topographic highs. When contrasted against cool local marine air that has isotopically heavier vapor with low *dxs* values, this produces the observed flip in summer correlations between isotopic species and temperature as well as the strengthened correlations with relative humidity.

Correlations between isotopes and water vapor mixing ratio greatly weaken in summer because mixing ratios do not clearly differentiate between local marine and southerly advected air. Although the shallow marine air has a higher relative humidity, it is also colder than the southerly advected air and thus has a lower maximum mixing ratio. In contrast, the relative humidity of southerly advected air is lower, but its warmer temperature means that the actual water content of the air can be very similar to that of local marine air. As a result, the relationship between temperature and mixing ratio decouples (Fig. S5), and isotopic correlations with mixing ratio also approach zero (Fig. 6b).

Two additional processes that emerge in summer may also lead to these relationship changes. First, the very warm conditions that occur during strong ridging over Greenland and enhanced southerly advection to Thule are also associated with intense surface melt and sublimation across the Tuto Ice Dome and greater Greenland Ice Sheet (Nghiem et al., 2012; van As et al., 2012; Neff et al., 2014; Ballinger et al., 2019). As the ice sheet surfaces are higher in elevation and colder than Thule, water vapor coming from their snow and glacial ice would be particularly isotopically light with high *dxs* values (Steen-Larsen et

https://doi.org/10.5194/acp-2020-340
Preprint. Discussion started: 18 May 2020


Atmospheric Chemistry and Physics Discussions

al., 2013; Kopec et al., 2014; Bréant et al., 2019), and this would enhance the isotopic signature of southerly advected air as it passes over the ice sheet on its way to Thule.

Second, the high pressure of these warm events often brings sunny weather to Thule that promotes intense heating of the local tundra and exposed rocky surfaces. For typical days outside of polar night, water vapor mixing ratio follows the daily temperature cycle and peaks in the early afternoon. However, on days when the mean temperature is greater than 10°C, the mixing ratio drops as temperature rises and hits its minimum daily value around local noon. This loss of water vapor suggests that daytime heating on the warmest days induces convection (Duynkerke and van den Broeke, 1994) that vertically mixes drier air aloft with lower $\delta^{18}O$ and $\delta^{2}H$ and higher *dxs* values (Bailey et al., 2013) down to the shallow marine surface layer, resulting in a net upward water vapor transport (Sherwood et al., 2010; Kiemle et al., 2013; Homeyer et al., 2014). The surface heating and drying during midday could also increase local evaporation of isotopically light water vapor from the land and surface waters.

6.4 Transition to winter and sea ice growth

The transition back to winter-type isotopic and meteorological conditions is much more gradual than spring breakup, in accordance with the relatively steady growth of sea ice. The $\delta^{18}O$ and δD values slowly decrease while *dxs* values slowly increase from October through November, and values through winter do not generally overlap summer values. While isotopic correlations with sea ice extent are near zero throughout summer (likely because any changes to sea ice extent at this time are occurring too far north to impact Thule), the autumnal growth of sea ice results in moderately strong correlations again in October (Fig. 6e) as the region of sea ice formation again affects Thule. Although small in magnitude, correlations with the NAO index also strengthen in autumn (Fig. 6f), and this is likely also due to the close relationship between NAO phase, sea ice extent, and local marine moisture availability. The return of true night brings a surface wind regime similar to that of spring, and correlations strengthen between isotopes and katabatic deviation until the sea breeze ceases due to polar night (Fig. 6d).

Interestingly, $\delta^{18}O$ and $\delta^{2}H$ have very strong positive correlations with sea ice extent in February and March, while *dxs* has very strong negative correlations with sea ice extent in February (Fig. 6e). These relationships are opposite to those observed in spring and autumn, when the presence or absence of sea ice plays a major role on local water availability. It is not entirely clear what is driving the strong correlations in late winter, as sea ice during these months is near its maximum extent and largely complete in coverage near Thule. The seasonal growth and loss of sea ice still dominates sea ice extent variability even when binned by month (unlike other variables with seasonal cycles like $\delta^{18}O$), and as a result, correlations with isotopes might simply reflect time of season instead. However, the general pattern and strength of monthly correlation strength remains the same even when sea ice extent values are seasonally-adjusted to remove the annual cycle.

These unusual correlations may then be due to coincidental extreme events. Shortly after the maximal extent of sea ice was reached in 2018, a major and extended moisture pulse event occurred which gave abnormally heavy water vapor isotopes with

https://doi.org/10.5194/acp-2020-340
Preprint. Discussion started: 18 May 2020


Atmospheric Chemistry and Physics Discussions

very low *dxs* values. While 2019 did not have an identified moisture pulse at maximal sea ice extent, the isotopes become unusually heavy with low *dxs* for two weeks (with an unclear cause) shortly after the sea ice peak. Because both periods in our record with the highest sea ice extent coincide with these events which isotopically resemble warmer conditions, it is difficult to conclude whether the observed correlative strengths in late winter are due simply to these two events or accurately represent a true change in isotopic character after a certain sea ice threshold is exceeded. Additional years of observation may help clarify this uncertainty.

7. Synoptic scale variability

Much of the daily and weekly isotopic variability at Thule can be attributed to the impacts of extratropical cyclones. These storm systems result in air mass changes that regularly shift $\delta^{18}O$ and *dxs* values by 5–10‰ as the warm sector brings isotopically heavier southerly advection and the cold sector supplies more fractionated and isotopically lighter moisture (Gedzelman and Lawrence, 1990; Coplen et al., 2008; Dütsch et al., 2016). The changes in temperature, surface winds, and cloud cover associated with cyclone passage also impact local water vapor isotopes altering rates of temperature-driven fractionation, local marine moisture sourcing, and evaposublimation. Over longer periods from seasons to years, changes in the mean NAO phase can shift the general storm track to enhance or suppress southerly advection and thus alter mean isotopic values.

During winter months, rapid shifts to extremely low NAO indices often coincide with intense poleward transport of southern heat and moisture to Thule that last 1–5 days. We refer to these distinct episodes as "moisture pulse events" as they appear very clearly in the Thule mixing ratio time series (Fig. 2). During these events, air temperature rises 10–15°C to peak near or above freezing and water vapor concentrations can reach four times greater than mean winter levels. These pulses appear to notably reduce or slow the growth of sea ice across Baffin Bay (Fig. 2j), although the sea ice stays largely intact in the northern reaches near Thule. Although not all these events meet the criteria of an atmospheric river (Mattingly et al., 2018), all have similar impacts to an atmospheric river event due to their anomalously high moisture and heat transport.

Unsurprisingly, such extreme weather changes are reflected by impressive water vapor isotopic responses. During a moisture pulse event, the $\delta^{18}O$ and δD rise 6–10‰ and 50–100‰, respectively, to reach values more typical of late spring and early summer. Concurrently, the *dxs* drops 15–25‰, and the minimum *dxs* values observed in these moisture pulse events match or exceed the minimum values observed at the height of summer. As sea ice coverage prevents the uptake of isotopically heavy/low *dxs* moisture from local waters during these moisture pulse events, the anomalous isotopic values must signify the presence of deep tropical or subtropical moisture transport (Bonne et al., 2015). A focused analysis of these events is currently underway.

The rapid isotopic and environmental shifts coinciding with sea ice break up in 2018 and 2019 also fit the general pattern of a moisture pulse event, but the variables do not return back to their preceding values after 1–5 days. Indeed, the shift in 2019 is

https://doi.org/10.5194/acp-2020-340
Preprint. Discussion started: 18 May 2020


Atmospheric Chemistry and Physics Discussions

associated with an atmospheric river event impacting western Greenland and an extreme drop in the NAO index from +2 to -2 while the 2018 shift coincided with an NAO index drop from +2.63 (the highest observed in our record) to +0.40 and an intense pulse of southerly moisture advection. In typical cold season moisture pulses, sea ice remains intact around Thule and the isotopic and meteorological effects from the southern moisture advection are short lived as the subtropical air mass moves on or mixes out. In these two spring events, however, local sea ice coverage is broken, and the new ample supply of local water vapor allows isotopic values to remain near those otherwise associated in winter with deep subtropical moisture.

8. Diel cycles

8.1 Diel cycles overview

Most polar sites report diel cycling of water vapor isotopes in summer (Steen-Larsen et al., 2013; Bastrikov et al., 2014; Bonne et al., 2014; Kopec et al., 2014; Casado et al., 2016; Ritter et al., 2016; Bréant et al., 2019), but attributed to different causes including katabatic wind cycling (Kopec et al., 2014; Bréant et al., 2019), vapor exchange between snow and air (Steen-Larsen et al., 2013; Casado et al., 2016), and dew formation (Bastrikov et al., 2014). In contrast to these sites, Thule exhibits relatively limited isotopic diel cycling in all months except March, with total cycle magnitudes less than 1‰ for both $\delta^{18}O$ and *dxs*, even when observations with possible cyclonic system impacts (i.e., lower than average station pressure) are excluded. Additionally, the existence of diel cycles is only evident when synoptic impacts are removed by averaging multiple days together. This subdued diel cycling is probably due to Thule's moderated coastal climate (Bréant et al., 2019; Bonne et al., 2020) and lengthy periods of midnight sun/polar night reduce the day-night contrasts that power diel cycles in weather and isotopic composition.

Looking broadly at the entire Thule isotopic record, the magnitude of isotopic diel cycles is not a significant driver of isotopic variability. However, we believe that analyzing these cycles gives better insight into the broader environmental controls on water vapor isotopes, including those at synoptic and annual scales. Based on observed isotopic and meteorological patterns, we divide diel cycles at Thule into four regimes: polar night, March, transition, and summer (Fig. 8). These regimes are superimposed on the broader seasonal changes in isotopic variability and control discussed previously. Out of the major drivers of isotopic change at Thule, air temperature, surface wind regime, and evaposublimation vary enough on hourly timescales to contribute to diel isotopic cycles, while synoptic pattern changes and sea ice extent are expressed at longer timeframes and/or not on a consistent daily cycle.

8.2 Polar night regime

The polar night regime includes the months from October through February, when daylight is very short (October, February) or nonexistent (November–January). With the lack of a strong insolation cycle, meteorological variables change little over a day, and winds are strong and consistently katabatic. Without any diel changes in the factors that drive isotopic change (i.e., air temperature, surface wind regimes, evaposublimation), the water vapor isotopes also show no diel cycling in the dark

https://doi.org/10.5194/acp-2020-340
Preprint. Discussion started: 18 May 2020


Atmospheric Chemistry and Physics Discussions

season. A slight hint of a rise or fall in values around local noon can be attributed to observations at the end of February that resemble the upcoming March regime.

8.3 March regime

The observed isotopic cycles in March (maximum diel range: $\delta^{18}O$: 2.4‰, δD: 16‰, *dxs*: 5.1‰) are by far the largest magnitude of any month of the year at Thule, although similar cycles with smaller amplitudes are also observed at the end of February. This heightened isotopic response appears due to several coinciding factors: a maximized daily insolation cycle near the equinox, an extensive snowpack to supply water vapor, and the enhanced impact of the snow-supplied vapor in the very dry environment (aided by the maximal seasonal extent of sea ice that limits external moisture input). This environment approximates the summer ice sheet setting of two other water vapor isotope observation sites, NEEM, Greenland (Steen-Larsen et al., 2013), and Dome C, Antarctica (Casado et al., 2016), and Thule's March isotopic diel regime appears similar to the cycles reported from those sites.

Moisture at Thule in March predominantly arrives from distant transport through katabatic flow with resulting low $\delta^{18}O$ and δD values and high *dxs* values. However, daytime heating of the snow surface across the landscape promotes release of water vapor held between snow grains that has have equilibrated with the local snow isotopes (Steen-Larsen et al., 2013; Casado et al., 2016). Because most snow in Thule falls in late autumn/early winter and is sourced from Baffin Bay, the equilibrated vapor will be isotopically heavier and have a lower *dxs* than the predominant external moisture arriving, producing the observed $\delta^{18}O$ and δD peak and *dxs* minimum around local noon. As insolation and air temperature drops in the evening, this vapor release ceases and potentially reverses, allowing the vapor isotopic composition to revert back to one of katabatic origin with lower $\delta^{18}O$ and δD and higher *dxs* values. The lack of a large drop in relative humidity coinciding with the midday temperature rise supports additional vapor is being supplied, and the local snowpack is the only likely source with all local waters frozen.

A similar isotopic regime does not reappear around the autumnal equinox due to a lack of extensive snowpack and a much higher water vapor content from warmer temperatures and open nearby seas that overwhelm the minor potential input from a snowpack vapor exchange. One exception, unique in the observed record, occurred from 20–25 September 2017 when an isotopic diel cycle very similar to March regime appeared (Fig. S6). This cycling occurred shortly after a snowfall and coincided with a diel surface wind cycle where the katabatic winds calmed each afternoon (though did not switch to a sea breeze). This appears to have allowed vapor released from the recent snow to raise isotopic values in the afternoon before the returning katabatic winds mixed the snow-derived moisture out and dropped isotopic values in the evening. In other September periods with a similar wind regime but without a recent snow cover, no isotopic cycling is observed.

https://doi.org/10.5194/acp-2020-340
Preprint. Discussion started: 18 May 2020


Atmospheric Chemistry and Physics Discussions

8.4 Summer regime

In the summer months (JJA), the midnight sun reduces the diel insolation cycle. Combined with the moderating influence of fully sea-ice free local seas, most meteorological variables are more stationary over the course of a day. With this reduced environmental variability, diel cycles in isotopes are subdued. The subtle daily patterns in $\delta^{18}O$ and *dxs* that do exist appear largely attributable to evaposublimation cycles: daily warming supplies low $\delta^{18}O$/high *dxs* water vapor through increased evaposublimation, with the resulting $\delta^{18}O$ maximum and *dxs* minimum around midday. However, we note that the magnitude of daily change (<0.5‰ for $\delta^{18}O$ and *dxs*) is largely within the confidence intervals of the mean.

Although the sea breeze has a diel cycle where it strengthens in the afternoon and weakens at night (Fig. 8g), there is not a clear binary switch back to full katabatic flow at night as observed at Kangerlussuaq (Kopec et al., 2014) and Dumont d'Urville (Bréant et al., 2019). This dominance of the sea breeze at Thule is likely due to 24 h summer insolation that can fuel a sea breeze even at "night". As a result, sea breeze-supplied local water is likely present throughout a typical day and night, and the nightly weakening of the sea breeze has limited isotopic effect without a full shift to katabatic flow.

8.5 Transition regime

The seasonal transition months of April, May, and September have a true day-night cycle that gives meteorological variables a greater diel amplitude than the summer or dark season. In contrast to March, these months are much warmer and humid, and moisture can be supplied from an open or opening Baffin Bay. Winds also exhibit a stronger diel cycle as surface heating leads to afternoon sea breeze development (Fig. 8g), but radiative heat loss over the ice sheet at night strengthens katabatic flow. We might expect a clear diel response in water vapor isotopes due to these heightened diel meteorological cycles, but the isotopes have little to no daily cycle.

While both the sea breeze and katabatic flow are likely sourcing similar southern moisture originating or passing over Baffin Bay, the sea breeze-sourced vapor coming directly off Bylot Sound in afternoon is isotopically heavier than the nighttime vapor that must travel over the Tuto Ice Dome and coastal mountains through katabatic flow. However, midday heating also increases the evaposublimation of surface waters and residual snow, and this vapor is isotopically lighter with high *dxs* values. The competing isotopic effects of the wind regime shifts and the evaposublimation cycle largely suppress any isotopic diel cycle from emerging, although the subtle late evening peak in $\delta^{18}O$ may arise because evaposublimation rates are reduced while the sea breeze is still ongoing.

9. Implications

The improved understanding of water vapor isotopic variability granted by our Thule observations can aid the interpretation of regional ice cores. The primary drivers of isotopic changes in water vapor are likely to also drive changes in local

https://doi.org/10.5194/acp-2020-340
Preprint. Discussion started: 18 May 2020


Atmospheric Chemistry and Physics Discussions

precipitation and accumulating snow, although there are many additional processes involved in the transfer of an isotopic signature from vapor to ice core that must be considered (Steen-Larsen et al., 2014; Casado et al., 2018; Madsen et al., 2019). Changes in $\delta^{18}O$ and δD have long been used to reconstruct climate change from deep Greenland ice cores, typically interpreted as local temperature variability (e.g., Dansgaard et al., 1969; Grootes and Stuiver, 1997; Johnsen et al., 2001). While air temperature is strongly correlated with isotopic change at Thule, much of this strength appears to arise as a common response between air temperature and sea ice extent to seasonal change. Air temperature might still be robustly reconstructed from isotopic archives based on our observed strong correlations, but the lack of a causative relationship risks misinterpretation if applied back far through time when the local environment may have significantly changed. Of particular warning is our observation that the basic relationship between temperature and water vapor isotopes inverts in summer, leading to very different isotopic interpretations depending on season. While this may be a local and/or coastal effect that is not expressed on ice sheets (Ballinger et al., 2019), we still advise caution.

More recently, additional consideration has been given to secondary isotopic variables like *dxs* and other environmental drivers such as moisture source, sea ice extent, and atmospheric circulation (e.g., Grumet et al., 2001; Vinther et al., 2003; Steffensen et al., 2008; Landais et al., 2018; Kopec et al., 2019). While our two-year Thule record is too short to statistically determine the strongest drivers of interannual isotopic variability, changes in the duration of sea ice coverage and mean NAO phase appear most likely to control year-to-year differences in mean isotopic composition. In line with recent interpretations in regional ice cores (Osterberg et al., 2015), our results suggest that past periods with decreased sea ice extent in Baffin Bay will have increased local marine moisture sourcing that produces higher $\delta^{18}O$ and δD and lower *dxs* values. In recent years, Baffin Bay has seen later sea ice freezes, earlier breakups, and a decrease in overall sea ice extent, attributing for 22% of recently observed loss in Arctic sea ice in March (Onarheim et al., 2018), and we expect such change to be isotopically preserved in future glacial ice as described. The future of the Nares ice bridge is one potential complication: should it consistently fail to form in a warmer world, the North Water Polynya may see increased sea ice cover that slows the overall sea ice impact on Thule (Barber et al., 2001; Puntsag et al., 2016; Vincent, 2019).

Losses in Arctic sea ice may also drive shifts in precipitation seasonality (Kopec et al., 2016) and atmospheric circulation (McLeod and Mote, 2016; Ballinger et al., 2018; Francis et al., 2018) that can alter the annual isotopic balance of precipitation. More open winter waters in Baffin Bay could decrease annual $\delta^{18}O$ and δD values as the relative fraction of isotopically lighter winter precipitation events increases, but this may be counter-balanced in part by the greater sourcing from isotopically heavy local waters. The extreme isotopic values we observe during moisture pulse events suggest that any changes in their frequency and magnitude (and more generally of related atmospheric river events) will have an outsized effect due to the sheer volume of moisture and precipitation they can bring to Greenland. For highly-resolved ice cores, it may be possible to identify particularly strong moisture pulse events as extreme minima in *dxs* values.

https://doi.org/10.5194/acp-2020-340
Preprint. Discussion started: 18 May 2020


Atmospheric Chemistry and Physics Discussions

Enhanced southerly moisture advection aided by NAO- conditions would also encourage higher $\delta^{18}O/\delta D$ and lower *dxs* periods in northwestern Greenland, though some caution might be warranted for complications from greater surface melt and vertical atmospheric mixing that we observed during summer NAO- phases. Additionally, the positive relationship between NAO phase and Baffin Bay sea ice extent (Mysak et al., 1996; Grumet et al., 2001; Stern and Heide-Jørgensen, 2003) makes it difficult to quantifiably split their influences on regional water isotopes. In the absence of additional clarifying evidence from other ice core proxies or nearby records, isotopic interpretations should be cautious in assigning cause solely to one factor or the other without further analysis to tease the factors apart.

10. Conclusions

Our two years of water vapor isotope monitoring in northwest Greenland have revealed a record of isotopic variability of unprecedented extent and resolution for High Arctic Greenland and one of the longest records of any polar site reported to date. The variability in water vapor isotopes at Thule is driven by five main interrelated environmental mechanisms: air temperature, moisture source, NAO/synoptic moisture transport, surface wind regimes, and evaposublimation. The relative importance of each mechanism changes over the course of the year and overall produces a clear annual isotopic cycle that is closely linked to sea ice extent in Baffin Bay. On top of these seasonal trends, mesoscale drivers such as sea breeze development, surface water/snow interactions, and convection can further modify the isotopic signature on diel cycles.

This analysis highlights the importance of local environment in isotope systematics. Compared to other high latitude water vapor isotope studies, Thule is more seriously impacted by sea ice fluctuations, both seasonal and interannual. Additionally, some of the finer-resolution controls that we have observed on isotopic variability, such as changes in relationship strength and direction during spring and summer, are so far uniquely reported for Thule. Thus, conclusions made from data at one high latitude site should not be applied indiscriminately to other sites without extensive validation that such a comparison is warranted.

Caution should also be made when making strong conclusions about isotopic controls based on observations of short duration (i.e., a single year or less). If data is only taken during a single season, any observed relationships may be specific only to that season and should not be assumed to be applicable to the entire year. For variables with relatively long-term variability, such as teleconnection indices, data from a single year is likely not long enough to reveal fully robust correlations. In our Thule data, we were fortunate that the synoptic patterns and NAO in 2018 and 2019 were different enough to allow analytical comparisons at monthly and seasonal resolutions. However, even two years of data are not enough to fully clarify the relationships between teleconnections and water vapor isotopes for all months, and we look forward to adding additional years of isotopic data in the future.

Moving forward, this isotope and meteorological database offers many opportunities for more in-depth and focused analyses of specific weather events and atmospheric patterns. As previously stated, our identified moisture pulse events are a focus of

https://doi.org/10.5194/acp-2020-340
Preprint. Discussion started: 18 May 2020


Atmospheric Chemistry and Physics Discussions

additional research, and we encourage the use of our data in other focused case studies. Water vapor isotope observations at Thule continue, and additional months and years of data will help refine and verify our conclusions made here. These results from Thule will help greatly in interpreting isotopic variability at other sites in the Arctic Water Isotope Network (Welker et al., 2019), and future collaborative analysis across this network will allow tracking the effects of synoptic weather patterns on water vapor isotopes in real time across the circumpolar region.

Data availability

Isotopic data is available at https://doi.org/10.18739/A21J9779S. Meteorological data for SMT is available at https://doi.org/10.1594/PANGAEA.895059 and in associated followup datasets by G. Muscari on PANGAEA. Meteorological data for THU is available upon request of the 821st Weather Squadron of the US Air Force.

Author contribution

JMW and ESK installed the L-2130i; PDA and BGK installed the dry air calibration system and performed maintenance on the L-2130i; PDA wrote the code in R for organizing and calibrating data and for statistical analyses; KSM performed back trajectory and water vapor transport analyses; DC performed cross-correlation analyses; PDA prepared the manuscript with contributions from all co-authors.

Competing interests

The authors declare that they have no conflict of interest.

Acknowledgments

This project was funded by NSF Arctic Observing Network-ITEX 1504141 and Arctic Observing Network- EAGER MOSAiC 1852614 and supported in part by the Inaugural UArctic Research Chairship to JMW. We greatly thank the assistance of the United States Air Force, the 821st Air Base Group at Thule Air Base, Vectrus, and Polar Field Services for logistical and hosting support throughout this research, and we thank Giovanni Muscari for graciously providing the SMT meteorological data. Special thanks go to the 821st weather squadron for meteorological data collection and to Shawn Arnett, Rich Biggins, Devin Brewer, Joe Burns, Matthew Burns, David Craig, Jarrod Dodgen, David Drainer, John Gaston, Missa Goldun, Pablo Londono, and Josh Neighbours for onsite assistance and maintenance. We also thank Matheiu Casado, Kazimierz Rozanski, and Hans Christian Steen-Larsen for their advice on isotopic calibration and interpretations.

https://doi.org/10.5194/acp-2020-340
Preprint. Discussion started: 18 May 2020

Atmospheric Chemistry and Physics Discussions

References

Addinsoft: XLSTAT statistical and data analysis solution, https://www.xlstat.com, 2020.

Aemisegger, F., Pfahl, S., Sodemann, H., Lehner, I., Seneviratne, S. I., and Wernli, H.: Deuterium excess as a proxy for continental moisture recycling and plant transpiration, Atmos. Chem. Phys., 14, 4029-4054, 2014.

Aemisegger, F.: On the link between the North Atlantic storm track and precipitation deuterium excess in Reykjavik, Atmos. Sci. Lett., 19, e865, 2018.

Aemisegger, F., and Papritz, L.: A climatology of strong large-scale ocean evaporation events. Part I: Identification, global distribution, and associated climate conditions, J. Clim., 31, 7287-7312, 2018.

Akers, P. D., Welker, J. M., and Brook, G. A.: Reassessing the role of temperature in precipitation oxygen isotopes across the eastern and central United States through weekly precipitation-day data, Water Resour. Res., 53, 7644-7661, 2017.

Atkinson, B. W.: Meso-scale atmospheric circulations, Academic Press, London, 495 pp., 1981.

Bailey, A., Toohey, D., and Noone, D.: Characterizing moisture exchange between the Hawaiian convective boundary layer and free troposphere using stable isotopes in water, J. Geophys. Res.-Atmos., 118, 8208-8221, 2013.

Bailey, A., Noone, D., Berkelhammer, M., Steen-Larsen, H. C., and Sato, P.: The stability and calibration of water vapor isotope ratio measurements during long-term deployments, Atmos. Meas. Tech., 8, 4521-4538, 10.5194/amt-8-4521-2015, 2015a.

Bailey, H. L., Kaufman, D. S., Henderson, A. C. G., and Leng, M. J.: Synoptic scale controls on the δ18O in precipitation across Beringia, Geophys. Res. Lett., 42, 4608-4616, 10.1002/2015gl063983, 2015b.

Ballinger, T. J., Hanna, E., Hall, R. J., Miller, J., Ribergaard, M. H., and Høyer, J. L.: Greenland coastal air temperatures linked to Baffin Bay and Greenland Sea ice conditions during autumn through regional blocking patterns, Clim. Dynam., 50, 83-100, 2018.

Ballinger, T. J., Mote, T. L., Mattingly, K., Bliss, A. C., Hanna, E., van As, D., Prieto, M., Gharehchahi, S., Fettweis, X., Noël, B., Smeets, P. C. J. P., Reijmer, C. H., Ribergaard, M. H., and Cappelen, J.: Greenland Ice Sheet late-season melt: investigating multiscale drivers of K-transect events, The Cryosphere, 13, 2241-2257, 2019.

Barber, D. G., Hanesiak, J. M., Chan, W., and Piwowar, J.: Sea-ice and meteorological conditions in Northern Baffin Bay and the North Water polynya between 1979 and 1996, Atmos. Ocean, 39, 343-359, 2001.

Bastrikov, V., Steen-Larsen, H. C., Masson-Delmotte, V., Gribanov, K., Cattani, O., Jouzel, J., and Zakharov, V.: Continuous measurements of atmospheric water vapour isotopes in western Siberia (Kourovka), Atmos. Meas. Tech., 7, 1763-1776, 10.5194/amt-7-1763-2014, 2014.

https://doi.org/10.5194/acp-2020-340
Preprint. Discussion started: 18 May 2020


Atmospheric Chemistry and Physics Discussions

Bhatt, U. S., Walker, D. A., Raynolds, M. K., Bieniek, P. A., Epstein, H. E., Comiso, J. C., Pinzon, J. E., Tucker, C. J., Steele, M., Ermold, W., and Zhang, J.: Changing seasonality of panarctic tundra vegetation in relationship to climatic variables, Environ. Res. Lett., 12, 055003, 2017.

Bjørk, A. A., Aagaard, S., Lütt, A., Khan, S. A., Box, J. E., Kjeldsen, K. K., Larsen, N. K., Korsgaard, N. J., Cappelen, J., Colgan, W. T., Machguth, H., Andresen, C. S., Peings, Y., and Kjær, K. H.: Changes in Greenland's peripheral glaciers linked to the North Atlantic Oscillation, Nat. Clim. Change, 8, 48-52, 2018.

Bonne, J. L., Masson-Delmotte, V., Cattani, O., Delmotte, M., Risi, C., Sodemann, H., and Steen-Larsen, H. C.: The isotopic composition of water vapour and precipitation in Ivittuut, southern Greenland, Atmos. Chem. Phys., 14, 4419-4439, 10.5194/acp-14-4419-2014, 2014.

Bonne, J. L., Steen-Larsen, H. C., Risi, C., Werner, M., Sodemann, H., Lacour, J. L., Fettweis, X., Cesana, G., Delmotte, M., Cattani, O., Vallelonga, P., Kjaer, H. A., Clerbaux, C., Sveinbjornsdottir, A. E., and Masson-Delmotte, V.: The summer 2012 Greenland heat wave: In situ and remote sensing observations of water vapor isotopic composition during an atmospheric river event, J. Geophys. Res.-Atmos., 120, 2970-2989, 10.1002/2014jd022602, 2015.

Bonne, J. L., Behrens, M., Meyer, H., Kipfstuhl, S., Rabe, B., Schonicke, L., Steen-Larsen, H. C., and Werner, M.: Resolving the controls of water vapour isotopes in the Atlantic sector, Nat. Comm., 10, 10.1038/s41467-019-09242-6, 2019.

Bonne, J. L., Meyer, H., Behrens, M., Boike, J., Kipfstuhl, S., Rabe, B., Schmidt, T., Schönicke, L., Steen-Larsen, H. C., and Werner, M.: Moisture origin as a driver of temporal variabilities of the water vapour isotopic composition in the Lena River Delta, Siberia, Atmos. Chem. Phys., 2020, 1-34, 2020.

Box, J. E., and Steffen, K.: Sublimation on the Greenland Ice Sheet from automated weather station observations, J. Geophys. Res.-Atmos., 106, 33965-33981, 10.1029/2001jd900219, 2001.

Box, J. E., Fettweis, X., Stroeve, J. C., Tedesco, M., Hall, D. K., and Steffen, K.: Greenland ice sheet albedo feedback: thermodynamics and atmospheric drivers, The Cryosphere, 6, 821-839, 2012.

Bréant, C., Dos Santos, C. L., Agosta, C., Casado, M., Fourre, E., Goursaud, S., Masson-Delmotte, V., Favier, V., Cattani, O., Prie, F., Golly, B., Orsi, A., Martinerie, P., and Landais, A.: Coastal water vapor isotopic composition driven by katabatic wind variability in summer at Dumont d'Urville, coastal East Antarctica, Earth and Planetary Science Letters, 514, 37-47, 10.1016/j.epsl.2019.03.004, 2019.

Carr, J. R., Vieli, A., and Stokes, C.: Influence of sea ice decline, atmospheric warming, and glacier width on marine-terminating outlet glacier behavior in northwest Greenland at seasonal to interannual timescales, J. Geophys. Res.-Earth, 118, 1210-1226, 10.1002/jgrf.20088, 2013.

https://doi.org/10.5194/acp-2020-340
Preprint. Discussion started: 18 May 2020

Casado, M., Landais, A., Masson-Delmotte, V., Genthon, C., Kerstel, E., Kassi, S., Arnaud, L., Picard, G., Prie, F., Cattani, O., Steen-Larsen, H. C., Vignon, E., and Cermak, P.: Continuous measurements of isotopic composition of water vapour on the East Antarctic Plateau, Atmos. Chem. Phys., 16, 8521-8538, 10.5194/acp-16-8521-2016, 2016.

Casado, M., Landais, A., Picard, G., Münch, T., Laepple, T., Stenni, B., Dreossi, G., Ekaykin, A., Arnaud, L., Genthon, C., Touzeau, A., Masson-Delmotte, V., and Jouzel, J.: Archival processes of the water stable isotope signal in East Antarctic ice cores, The Cryosphere, 12, 1745-1766, 2018.

Castro de la Guardia, L., Hu, X., and Myers, P. G.: Potential positive feedback between Greenland Ice Sheet melt and Baffin Bay heat content on the west Greenland shelf, Geophys. Res. Lett., 42, 4922-4930, 10.1002/2015gl064626, 2015.

Chen, Q., Bromwich, D. H., and Bai, L.: Precipitation over Greenland retrieved by a dynamic method and its relation to cyclonic activity, J. Clim., 10, 839-870, 10.1175/1520-0442(1997)010<0839:pogrba>2.0.co;2, 1997.

Cohen, J., Zhang, X., Francis, J., Jung, T., Kwok, R., Overland, J., Ballinger, T. J., Bhatt, U. S., Chen, H. W., Coumou, D., Feldstein, S., Gu, H., Handorf, D., Henderson, G., Ionita, M., Kretschmer, M., Laliberte, F., Lee, S., Linderholm, H. W., Maslowski, W., Peings, Y., Pfeiffer, K., Rigor, I., Semmler, T., Stroeve, J., Taylor, P. C., Vavrus, S., Vihma, T., Wang, S., Wendisch, M., Wu, Y., and Yoon, J.: Divergent consensuses on Arctic amplification influence on midlatitude severe winter weather, Nat. Clim. Change, 10, 20-29, 2020.

Coplen, T. B., Neiman, P. J., White, A. B., Landwehr, J. M., Ralph, F. M., and Dettinger, M. D.: Extreme changes in stable hydrogen isotopes and precipitation characteristics in a landfalling Pacific storm, Geophys. Res. Lett., 35, 2008.

Craig, H.: Isotopic variations in meteoric waters, Science, 133, 1702, 1961.

Csank, A. Z., Czimczik, C. I., Xu, X., and Welker, J. M.: Seasonal patterns of riverine carbon sources and export in NW Greenland, J. Geophys. Res.-Biogeo., 124, 840-856, 2019.

Dansgaard, W.: Stable isotopes in precipitation, Tellus, 16, 436-468, 1964.

Dansgaard, W., Johnsen, S. J., Møller, J., and Langway, C. C.: One thousand centuries of climatic record from Camp Century on the Greenland Ice Sheet, Science, 166, 377, 1969.

Dütsch, M., Pfahl, S., and Wernli, H.: Drivers of δ2H variations in an idealized extratropical cyclone, Geophys. Res. Lett., 43, 5401-5408, 2016.

Dütsch, M., Pfahl, S., and Sodemann, H.: The impact of nonequilibrium and equilibrium fractionation on two different deuterium excess definitions, J. Geophys. Res.-Atmos., 122, 12,732-712,746, 10.1002/2017jd027085, 2017.

Duynkerke, P. G., and van den Broeke, M. R.: Surface energy balance and katabatic flow over glacier and tundra during GIMEX-91, Greenland ice margin experiment (GIMEx), 9, 17-28, 1994.

https://doi.org/10.5194/acp-2020-340
Preprint. Discussion started: 18 May 2020


Atmospheric Chemistry and Physics Discussions

Farquhar, G. D., Cernusak, L. A., and Barnes, B.: Heavy water fractionation during transpiration, Plant Physiol., 143, 11, 2007.

Feng, X., Faiia, A. M., and Posmentier, E. S.: Seasonality of isotopes in precipitation: A global perspective, J. Geophys. Res.-Atmos., 114, 2009.

Fetterer, F., Savoie, M., Helfrich, S., and Clemente-Colón, P.: Multisensor Analyzed Sea Ice Extent - Northern Hemisphere (MASIE-NH), Version 1, NSIDC: National Snow and Ice Data Center, https://doi.org/10.7265/N5GT5K3K, 2010.

Fetterer, F., Knowles, K., Meier, W. N., Savoie, M., and Windnagel, A. K.: Sea Ice Index, Version 3. Extent, Concentration, and Concentration Anomalies, NSIDC: National Snow and Ice Data Center, https://doi.org/10.7265/N5K072F8, 2017.

Francis, J. A., and Vavrus, S. J.: Evidence linking Arctic amplification to extreme weather in mid-latitudes, Geophys. Res. Lett., 39, 10.1029/2012gl051000, 2012.

Francis, J. A., Skific, N., and Vavrus, S. J.: North American weather regimes are becoming more persistent: Is Arctic Amplification a factor?, Geophys. Res. Lett., 45, 11,414-411,422, 10.1029/2018gl080252, 2018.

Gat, J. R., and Matsui, E.: Atmospheric water balance in the Amazon basin: An isotopic evapotranspiration model, J. Geophys. Res.-Atmos., 96, 13179-13188, 10.1029/91jd00054, 1991.

Gat, J. R.: Oxygen and hydrogen isotopes in the hydrologic cycle, Annu. Rev. Earth Pl. Sc., 24, 225-262, 1996.

Gedzelman, S. D., and Lawrence, J. R.: The isotopic composition of precipitation from two extratropical cyclones, Mon. Weather Rev., 118, 495-509, 1990.

Gelaro, R., McCarty, W., Suárez, M. J., Todling, R., Molod, A., Takacs, L., Randles, C. A., Darmenov, A., Bosilovich, M. G., Reichle, R., Wargan, K., Coy, L., Cullather, R., Draper, C., Akella, S., Buchard, V., Conaty, A., da Silva, A. M., Gu, W., Kim, G.-K., Koster, R., Lucchesi, R., Merkova, D., Nielsen, J. E., Partyka, G., Pawson, S., Putman, W., Rienecker, M., Schubert, S. D., Sienkiewicz, M., and Zhao, B.: The Modern-Era Retrospective Analysis for Research and Applications, Version 2 (MERRA-2), J. Clim., 30, 5419-5454, 2017.

Gimeno, L., Vázquez, M., Eiras-Barca, J., Sorí, R., Algarra, I., and Nieto, R.: Atmospheric moisture transport and the decline in Arctic Sea ice, WIRES Clim. Change, 10, e588, 10.1002/wcc.588, 2019.

Gold, W. G., and Bliss, L. C.: Water limitations and plant community development in a polar desert, Ecology, 76, 1558-1568, 1995.

Grootes, P. M., and Stuiver, M.: Oxygen 18/16 variability in Greenland snow and ice with 10(-3)- to 10(5)-year time resolution, J. Geophys. Res.-Oceans, 102, 26455-26470, 10.1029/97JC00880, 1997.

Grumet, N. S., Wake, C. P., Mayewski, P. A., Zielinski, G. A., Whitlow, S. I., Koerner, R. M., Fisher, D. A., and Woollett, J. M.: Variability of sea-ice extent in Baffin Bay over the last millennium, Clim. Change, 49, 129-145, 2001.

https://doi.org/10.5194/acp-2020-340
Preprint. Discussion started: 18 May 2020


Atmospheric Chemistry and Physics Discussions

Gurney, S. D., and Lawrence, D. S. L.: Seasonal trends in the stable isotopic composition of snow and meltwater runoff in a subarctic catchment at Okstindan, Norway, Nord. Hydrol., 35, 119-137, 2004.

Hall, D. K., and Riggs, G. A.: MODIS/Aqua Sea Ice Extent Daily L3 Global 1km EASE-Grid Day, Version 6, NASA NSIDC Distributed Active Archive Center, https://doi.org/10.5067/MODIS/MYD29P1D.006, 2015.

Heide-Jørgensen, M. P., Sinding, M. H. S., Nielsen, N. H., Rosing-Asvid, A., and Hansen, R. G.: Large numbers of marine mammals winter in the North Water polynya, Polar Biol., 39, 1605-1614, 2016.

Homeyer, C. R., Pan, L. L., Dorsi, S. W., Avallone, L. M., Weinheimer, A. J., O'Brien, A. S., DiGangi, J. P., Zondlo, M. A., Ryerson, T. B., Diskin, G. S., and Campos, T. L.: Convective transport of water vapor into the lower stratosphere observed during double-tropopause events, J. Geophys. Res.-Atmos., 119, 10,941-910,958, 2014.

Hooke, R. L.: Morphology of the ice-sheet margin near Thule, Greenland, J. Glaciol., 9, 303-324, 1970.

Howat, I.: MEaSUREs Greenland Ice Mapping Project (GIMP) Land Ice and Ocean Classification Mask, Version 1, 90 m x 90 m, NASA NSIDC Distributed Active Archive Center, https://doi.org/10.5067/B8X58MQBFUPA, 2017.

Howat, I. M., Negrete, A., and Smith, B. E.: The Greenland Ice Mapping Project (GIMP) land classification and surface elevation data sets, The Cryosphere, 8, 1509-1518, 2014.

IPCC: Climate Change 2014: Synthesis Report. Contribution of Working Groups I, II and III to the Fifth Assessment Report of the Intergovernmental Panel on Climate Change, 2014.

Johnsen, S. J., Dahl-Jensen, D., Gundestrup, N., Steffensen, J. P., Clausen, H. B., Miller, H., Masson-Delmotte, V., Sveinbjörnsdottir, A. E., and White, J.: Oxygen isotope and palaeotemperature records from six Greenland ice-core stations: Camp Century, Dye-3, GRIP, GISP2, Renland and NorthGRIP, J. Quaternary Sci., 16, 299-307, 2001.

Jouzel, J., and Merlivat, L.: Deuterium and oxygen 18 in precipitation: Modeling of the isotopic effects during snow formation, J. Geophys. Res.-Atmos., 89, 11749-11757, 10.1029/JD089iD07p11749, 1984.

Kiemle, C., Schäfler, A., Wirth, M., Fix, A., and Rahm, S.: Detection and analysis of water vapor transport by airborne lidars, IEEE J. Sel. Top. Appl, 6, 1189-1193, 2013.

Klein, E. S., Cherry, J. E., Young, J., Noone, D., Leffler, A. J., and Welker, J. M.: Arctic cyclone water vapor isotopes support past sea ice retreat recorded in Greenland ice, Scientific Reports, 5, 10.1038/srep10295, 2015.

Klein, E. S., and Welker, J. M.: Influence of sea ice on ocean water vapor isotopes and Greenland ice core records, Geophys. Res. Lett., 43, 12475-12483, 10.1002/2016GL071748, 2016.

Kopec, B. G., Lauder, A. M., Posmentier, E. S., and Feng, X.: The diel cycle of water vapor in west Greenland, J. Geophys. Res.-Atmos., 119, 9386-9399, 2014.

https://doi.org/10.5194/acp-2020-340
Preprint. Discussion started: 18 May 2020


Atmospheric Chemistry and Physics Discussions

Kopec, B. G., Feng, X., Michel, F. A., and Posmentier, E. S.: Influence of sea ice on Arctic precipitation, P. Natl. A. Sci., 113, 46, 2016.

Kopec, B. G., Feng, X., Posmentier, E. S., and Sonder, L. J.: Seasonal deuterium excess variations of precipitation at Summit, Greenland, and their climatological significance, J. Geophys. Res.-Atmos., 124, 72-91, 10.1029/2018JD028750, 2019.

Kurita, N.: Origin of Arctic water vapor during the ice-growth season, Geophys. Res. Lett., 38, 10.1029/2010GL046064, 2011.

Laidre, K. L., Atkinson, S., Regehr, E. V., Stern, H. L., Born, E. W., Wiig, Ø., Lunn, N. J., and Dyck, M.: Interrelated ecological impacts of climate change on an apex predator, Ecol. Appl., n/a, 10.1002/eap.2071, 2020.

Landais, A., Capron, E., Masson-Delmotte, V., Toucanne, S., Rhodes, R., Popp, T., Vinther, B., Minster, B., and Prié, F.: Ice core evidence for decoupling between midlatitude atmospheric water cycle and Greenland temperature during the last deglaciation, Clim. Past, 14, 1405-1415, 2018.

Leffler, A. J., and Welker, J. M.: Long-term increases in snow pack elevate leaf N and photosynthesis in Salix arctica : responses to a snow fence experiment in the High Arctic of NW Greenland, Environ. Res. Lett., 8, 025023, 2013.

Liu, C., and Barnes, E. A.: Extreme moisture transport into the Arctic linked to Rossby wave breaking, J. Geophys. Res.-Atmos., 120, 3774-3788, 10.1002/2014jd022796, 2015.

Madsen, M. V., Steen-Larsen, H. C., Hoerhold, M., Box, J., Berben, S. M. P., Capron, E., Faber, A. K., Hubbard, A., Jensen, M. F., Jones, T. R., Kipfstuhl, S., Koldtoft, I., Pillar, H. R., Vaughn, B. H., Vladimirova, D., and Dahl-Jensen, D.: Evidence of isotopic fractionation during vapor exchange between the atmosphere and the snow surface in Greenland, J. Geophys. Res.-Atmos., 124, 2932-2945, 10.1029/2018jd029619, 2019.

Maslanik, J., and Stroeve, J.: Near-Real-Time DMSP SSM/I-SSMIS Daily Polar Gridded Brightness Temperatures, Version 1, NASA NSIDC Distributed Active Archive Center, https://doi.org/10.5067/AKQDND71ZDLF, 1999.

Mastenbrook, H. J.: Water vapor distribution in the stratosphere and high troposphere, J. Atmos. Sci., 25, 299-311, 10.1175/1520-0469(1968)025<0299:wvdits>2.0.co;2, 1968.

Mattingly, K. S., Mote, T. L., and Fettweis, X.: Atmospheric river impacts on Greenland Ice Sheet surface mass balance, J. Geophys. Res.-Atmos., 123, 8538-8560, 10.1029/2018jd028714, 2018.

McLeod, J. T., and Mote, T. L.: Linking interannual variability in extreme Greenland blocking episodes to the recent increase in summer melting across the Greenland ice sheet, Int. J. Climatol., 36, 1484-1499, 2016.

Meier, W. N., Stroeve, J., and Gearheard, S.: Bridging perspectives from remote sensing and Inuit communities on changing sea-ice cover in the Baffin Bay region, Ann. Glaciol., 44, 433-438, 2006.

Molina, M. J., and Allen, J. T.: On the moisture origins of tornadic thunderstorms, J. Clim., 32, 4321-4346, 2019.

Moore, G. W. K.: The March 1972 northwest Greenland windstorm: evidence of downslope winds associated with a trapped lee wave, Q. J. Roy. Meteor. Soc., 142, 1428-1438, 10.1002/qj.2744, 2016.

Moorman, B. J., Michel, F. A., and Drimmie, R. J.: Isotopic variability in Arctic precipitation as a climatic indicator, Geosci. Can., 23, 1996.

MOSAiC: Multidisciplinary drifting Observatory for the Study of Arctic Climate (MOSAiC) Project: https://mosaic-expedition.org/, 2020.

Muscari, G.: Ground meteorological data (T, P, RH) obtained during the YOPP SOP in early 2018 at Thule Air Base, Greenland, Istituto Nazionale di Geofisica e Vulcanologia, Roma, Italy, PANGAEA, https://doi.org/10.1594/PANGAEA.895059, 2018, and related Muscari datasets also on PANGAEA.

Mysak, L. A., Ingram, R. G., Wang, J., and van der Baaren, A.: The anomalous sea-ice extent in Hudson bay, Baffin bay and the Labrador sea during three simultaneous NAO and ENSO episodes, Atmos. Ocean, 34, 313-343, 1996.

Neff, W., Compo, G. P., Martin, R. F., and Shupe, M. D.: Continental heat anomalies and the extreme melting of the Greenland ice surface in 2012 and 1889, J. Geophys. Res.-Atmos., 119, 6520-6536, 10.1002/2014jd021470, 2014.

Nghiem, S. V., Hall, D. K., Mote, T. L., Tedesco, M., Albert, M. R., Keegan, K., Shuman, C. A., DiGirolamo, N. E., and Neumann, G.: The extreme melt across the Greenland ice sheet in 2012, Geophys. Res. Lett., 39, 10.1029/2012gl053611, 2012.

NOAA: Climate Prediction Center: Teleconnections - Archive of Daily Indices, NOAA National Weather Service, https://www.cpc.ncep.noaa.gov/products/precip/CWlink/daily_ao_index/teleconnections.shtml, 2019.

NOAA: Arctic Report Card, NOAA Arctic Program, https://arctic.noaa.gov/, 2020.

Noël, B., van de Berg, W. J., Lhermitte, S., and van den Broeke, M. R.: Rapid ablation zone expansion amplifies north Greenland mass loss, Sci Adv, 5, 2019.

Nusbaumer, J., Alexander, P. M., LeGrande, A. N., and Tedesco, M.: Spatial shift of Greenland moisture sources related to enhanced Arctic warming, Geophys. Res. Lett., 46, 14723-14731, 10.1029/2019gl084633, 2019.

Olden, J. D., and Neff, B. D.: Cross-correlation bias in lag analysis of aquatic time series, Mar. Biol., 138, 1063-1070, 2001.

Oltmanns, M., Straneo, F., and Tedesco, M.: Increased Greenland melt triggered by large-scale, year-round cyclonic moisture intrusions, The Cryosphere, 13, 815-825, 10.5194/tc-13-815-2019, 2019.

Onarheim, I. H., Eldevik, T., Smedsrud, L. H., and Stroeve, J. C.: Seasonal and regional manifestation of Arctic sea ice loss, J. Clim., 31, 4917-4932, 2018.

Osterberg, E. C., Hawley, R. L., Wong, G., Kopec, B., Ferris, D., and Howley, J.: Coastal ice-core record of recent northwest Greenland temperature and sea-ice concentration, J. Glaciol., 61, 1137-1146, 2015.

Peterson, T. C., Karl, T. R., Jamason, P. F., Knight, R., and Easterling, D. R.: First difference method: Maximizing station density for the calculation of long-term global temperature change, J. Geophys. Res.-Atmos., 103, 25967-25974, 10.1029/98jd01168, 1998.

Petrie, R. E., Shaffrey, L. C., and Sutton, R. T.: Atmospheric response in summer linked to recent Arctic sea ice loss, Q. J. Roy. Meteor. Soc., 141, 2070-2076, 2015.

Pfahl, S., and Sodemann, H.: What controls deuterium excess in global precipitation?, Clim. Past, 10, 771-781, 2014.

Pithan, F., Svensson, G., Caballero, R., Chechin, D., Cronin, T. W., Ekman, A. M. L., Neggers, R., Shupe, M. D., Solomon, A., Tjernström, M., and Wendisch, M.: Role of air-mass transformations in exchange between the Arctic and mid-latitudes, Nat. Geosci., 11, 805-812, 2018.

Porter, C., Morin, P., Howat, I., Noh, M. J., Bates, B., Peterman, K., Keesey, S., Schlenk, M., Gardiner, J., Tomko, K., Willis, M., Kelleher, C., Cloutier, M., Husby, E., Foga, S., Nakamura, H., Platson, M., Wethington, M., Williamson, C., Bauer, G., Enos, J., Arnold, G., Kramer, W., Becker, P., Doshi, A., D'Souza, C., Cummens, P., Laurier, F., and Bojesen, M.: ArcticDEM, V1, https://doi.org/10.7910/DVN/OHHUKH, 2018.

Puntsag, T., Mitchell, M. J., Campbell, J. L., Klein, E. S., Likens, G. E., and Welker, J. M.: Arctic Vortex changes alter the sources and isotopic values of precipitation in northeastern US, Scientific Reports, 6, 22647, 2016.

Putman, A. L., Feng, X. H., Sonder, L. J., and Posmentier, E. S.: Annual variation in event-scale precipitation delta H-2 at Barrow, AK, reflects vapor source region, Atmos. Chem. Phys., 17, 4627-4639, 10.5194/acp-17-4627-2017, 2017.

Reeh, N., Thomsen, H. H., Frich, P., and Clausen, H. B.: Stable isotope studies on ice margins in the Thule area, in: Late Quaternary stratigraphy and glaciology in the Thule area, Northwest Greenland, edited by: Funder, S., Meddelelser Om Grønland, Geosicence, 47-56, 1990.

Ritter, F., Steen-Larsen, H. C., Werner, M., Masson-Delmotte, V., Orsi, A., Behrens, M., Birnbaum, G., Freitag, J., Risi, C., and Kipfstuhl, S.: Isotopic exchange on the diurnal scale between near-surface snow and lower atmospheric water vapor at Kohnen station, East Antarctica, The Cryosphere, 10, 1647-1663, 2016.

Rogers, M. C., Sullivan, P. F., and Welker, J. M.: Evidence of nonlinearity in the response of net ecosystem CO2 exchange to increasing levels of winter snow depth in the High Arctic of Northwest Greenland, Arct. Antarct. Alp. Res., 43, 95-106, 2011.

Rozanski, K., Araguás-Araguás, L., and Gonfiantini, R.: Isotopic patterns in modern global precipitation, Climate Change in Continental Isotopic Records, 1-36, 1993.

https://doi.org/10.5194/acp-2020-340
Preprint. Discussion started: 18 May 2020

Runge, J., Petoukhov, V., and Kurths, J.: Quantifying the strength and delay of climatic interactions: The ambiguities of cross correlation and a novel measure based on graphical models, J. Clim., 27, 720-739, 10.1175/jcli-d-13-00159.1, 2014.

Schaeffer, S. M., Sharp, E., Schimel, J. P., and Welker, J. M.: Soil–plant N processes in a High Arctic ecosystem, NW Greenland are altered by long-term experimental warming and higher rainfall, Global Change Biol., 19, 3529-3539, 10.1111/gcb.12318, 2013.

Schytt, V.: Glaciological investigations in the Thule Ramp area, Report of the Cold Regions Research and Engineering Laboratory, 28, 88, 1955.

Sherwood, S. C., Roca, R., Weckwerth, T. M., and Andronova, N. G.: Tropospheric water vapor, convection, and climate, Rev. Geophys., 48, 2010.

Sodemann, H., Schwierz, C., and Wernli, H.: Interannual variability of Greenland winter precipitation sources: Lagrangian moisture diagnostic and North Atlantic Oscillation influence, J. Geophys. Res.-Atmos., 113, 10.1029/2007jd008503, 2008.

Stansfield, J. R.: The severe Arctic Storm of 8–9 March 1972 at Thule Air Force Base, Greenland, Weatherwise, 25, 228-232, 1972.

Steen-Larsen, H. C., Johnsen, S. J., Masson-Delmotte, V., Stenni, B., Risi, C., Sodemann, H., Balslev-Clausen, D., Blunier, T., Dahl-Jensen, D., Ellehoj, M. D., Falourd, S., Grindsted, A., Gkinis, V., Jouzel, J., Popp, T., Sheldon, S., Simonsen, S. B., Sjolte, J., Steffensen, J. P., Sperlich, P., Sveinbjornsdottir, A. E., Vinther, B. M., and White, J. W. C.: Continuous monitoring of summer surface water vapor isotopic composition above the Greenland Ice Sheet, Atmos. Chem. Phys., 13, 4815-4828, 10.5194/acp-13-4815-2013, 2013.

Steen-Larsen, H. C., Masson-Delmotte, V., Hirabayashi, M., Winkler, R., Satow, K., Prie, F., Bayou, N., Brun, E., Cuffey, K. M., Dahl-Jensen, D., Dumont, M., Guillevic, M., Kipfstuhl, S., Landais, A., Popp, T., Risi, C., Steffen, K., Stenni, B., and Sveinbjornsdottir, A. E.: What controls the isotopic composition of Greenland surface snow?, Clim. Past, 10, 377-392, 10.5194/cp-10-377-2014, 2014.

Steffensen, J. P., Andersen, K. K., Bigler, M., Clausen, H. B., Dahl-Jensen, D., Fischer, H., Goto-Azuma, K., Hansson, M., Johnsen, S. J., Jouzel, J., Masson-Delmotte, V., Popp, T., Rasmussen, S. O., Röthlisberger, R., Ruth, U., Stauffer, B., Siggaard-Andersen, M. L., Sveinbjörnsdóttir, Á. E., Svensson, A., and White, J. W. C.: High-resolution Greenland ice core data show abrupt climate change happens in few years, Science, 321, 680-684, 10.1126/science.1157707, 2008.

Stein, A. F., Draxler, R. R., Rolph, G. D., Stunder, B. J. B., Cohen, M. D., and Ngan, F.: NOAA's HYSPLIT atmospheric transport and dispersion modeling system, B. Am. Meteorol. Soc., 96, 2059-2077, 2015.

Stern, H. L., and Heide-Jørgensen, M. P.: Trends and variability of sea ice in Baffin Bay and Davis Strait, 1953–2001, Polar Res., 22, 11-18, 10.1111/j.1751-8369.2003.tb00090.x, 2003.

https://doi.org/10.5194/acp-2020-340
Preprint. Discussion started: 18 May 2020

Stroeve, J., and Meier, W. N.: Sea ice trends and climatologies from SMMR and SSM/I-SSMIS, Version 3, NASA NSIDC Distributed Active Archive Center, https://doi.org/10.5067/IJ0T7HFHB9Y6, 2018.

Sullivan, P. F., Welker, J. M., Steltzer, H., Sletten, R. S., Hagedorn, B., Arens, S. J. T., and Horwath, J. L.: Energy and water additions give rise to simple responses in plant canopy and soil microclimates of a high arctic ecosystem, J. Geophys. Res.-Biogeo., 113, 2008.

Tang, C. C. L., Ross, C. K., Yao, T., Petrie, B., DeTracey, B. M., and Dunlap, E.: The circulation, water masses and sea-ice of Baffin Bay, Prog. Oceanogr., 63, 183-228, 2004.

Tedesco, M., and Fettweis, X.: Unprecedented atmospheric conditions (1948–2019) drive the 2019 exceptional melting season over the Greenland ice sheet, The Cryosphere Discuss., 2019, 1-26, 2019.

Theakstone, W. H.: A seven-year study of oxygen isotopes in daily precipitation at a site close to the Arctic Circle, Tustervatn, Norway: Trajectory analysis and links with the North Atlantic Oscillation, Atmos. Environ., 45, 5101-5109, 2011.

USAF: THU weather observations, Thule Air Base, Greenland, 821 SPTS/OSW, USAF, 2019.

van As, D.: Warming, glacier melt and surface energy budget from weather station observations in the Melville Bay region of northwest Greenland, J. Glaciol., 57, 208-220, 2011.

van As, D., Hubbard, A. L., Hasholt, B., Mikkelsen, A. B., van den Broeke, M. R., and Fausto, R. S.: Large surface meltwater discharge from the Kangerlussuaq sector of the Greenland ice sheet during the record-warm year 2010 explained by detailed energy balance observations, The Cryosphere, 6, 199-209, 10.5194/tc-6-199-2012, 2012.

van As, D., Fausto, R. S., Steffen, K., and Team, P. P.: Katabatic winds and piteraq storms: observations from the Greenland ice sheet, Geol. Surv. Den. Greenl., 83-86, 2014.

Vihma, T., Screen, J., Tjernstrom, M., Newton, B., Zhang, X., Popova, V., Deser, C., Holland, M., and Prowse, T.: The atmospheric role in the Arctic water cycle: A review on processes, past and future changes, and their impacts, J. Geophys. Res.-Biogeo., 121, 586-620, 10.1002/2015jg003132, 2016.

Vincent, R. F.: A Study of the North Water Polynya Ice Arch using four decades of satellite data, Scientific Reports, 9, 20278, 2019.

Vinther, B. M., Johnsen, S. J., Andersen, K. K., Clausen, H. B., and Hansen, A. W.: NAO signal recorded in the stable isotopes of Greenland ice cores, Geophys. Res. Lett., 30, 10.1029/2002gl016193, 2003.

Vinther, B. M., Jones, P. D., Briffa, K. R., Clausen, H. B., Andersen, K. K., Dahl-Jensen, D., and Johnsen, S. J.: Climatic signals in multiple highly resolved stable isotope records from Greenland, Quaternary Sci. Rev., 29, 522-538, 2010.

https://doi.org/10.5194/acp-2020-340
Preprint. Discussion started: 18 May 2020

Warner, M. S. C.: Introduction to PySPLIT: A Python Toolkit for NOAA ARL's HYSPLIT Model, Comput. Sci. Eng., 20(5), 47-62, 10.1109/MCSE.2017.3301549, 2018.

Welker, J. M.: Isotopic (δ18O) characteristics of weekly precipitation collected across the USA: an initial analysis with application to water source studies, Hydrol. Process., 14, 1449-1464, 2000.

Welker, J. M., Rayback, S., and Henry, G. H. R.: Arctic and North Atlantic Oscillation phase changes are recorded in the isotopes (δ18O and δ13C) of Cassiope tetragona plants, Global Change Biol., 11, 997-1002, 10.1111/j.1365-2486.2005.00961.x, 2005.

Welker, J. M., Klein, E. S., Noone, D., Bailey, H., Akers, P. D., Kopec, B. G., Marttila, H., Mustonen, K. R., Kløve, B., and Steen-Larsen, H. C.: MOSAiC's Pan Arctic water isotope network & discoveries, American Geophysical Union Fall Meeting, San Francisco, CA, USA, 2019.

Wille, J. D., Favier, V., Dufour, A., Gorodetskaya, I. V., Turner, J., Agosta, C., and Codron, F.: West Antarctic surface melt triggered by atmospheric rivers, Nat. Geosci., 12, 911-916, 2019.

Woods, C., Caballero, R., and Svensson, G.: Large-scale circulation associated with moisture intrusions into the Arctic during winter, Geophys. Res. Lett., 40, 4717-4721, 10.1002/grl.50912, 2013.

Zheng, M., Sjolte, J., Adolphi, F., Vinther, B. M., Steen-Larsen, H. C., Popp, T. J., and Muscheler, R.: Climate information preserved in seasonal water isotope at NEEM: relationships with temperature, circulation and sea ice, Clim. Past, 14, 1067-1078, 2018.

https://doi.org/10.5194/acp-2020-340
Preprint. Discussion started: 18 May 2020

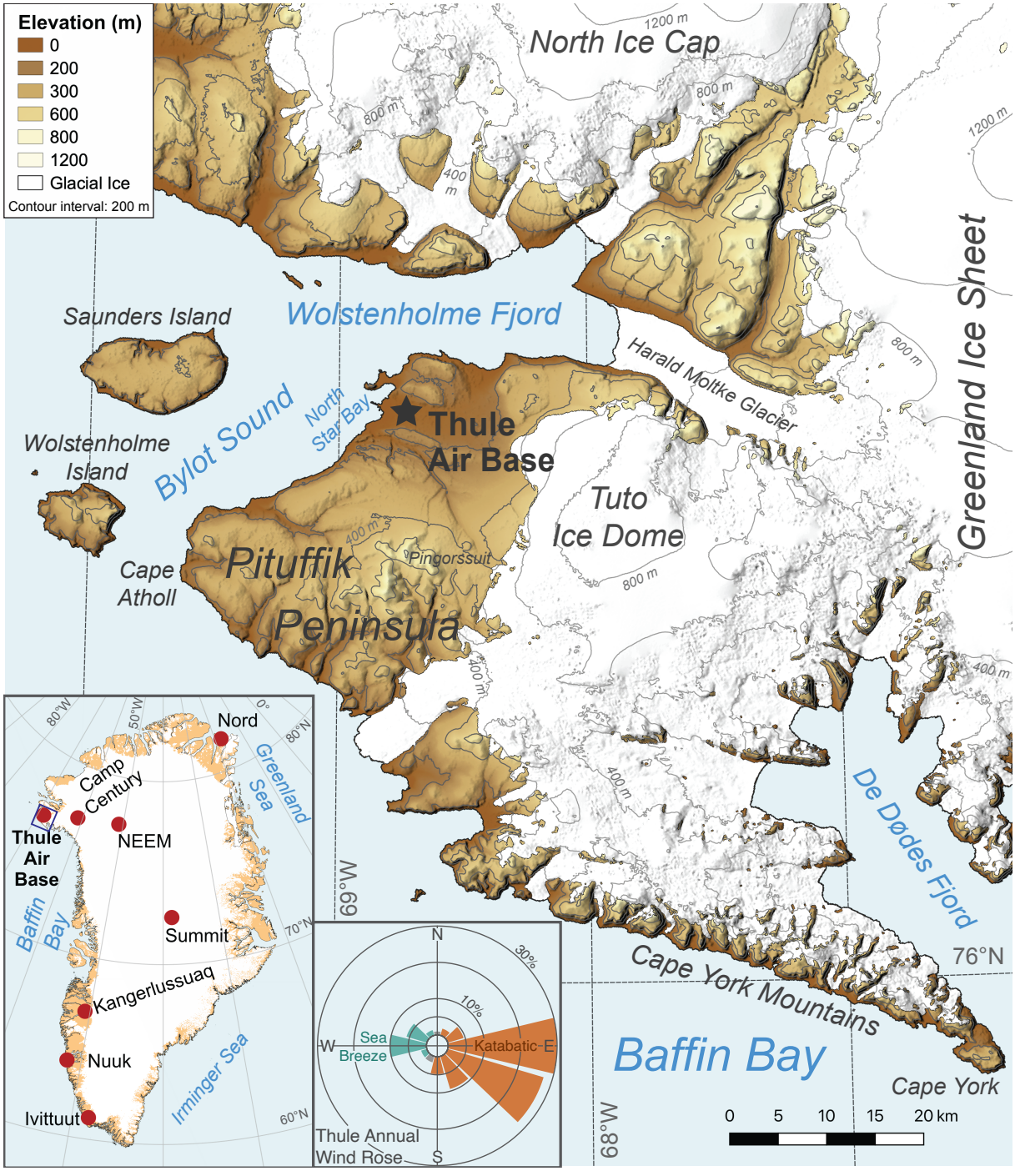

Figure 1. Map of the local geography around Thule Air Base, site of water vapor and meteorological measurements. The inset map shows the location of Thule Air Base in Greenland and other important and/or related Greenland. Elevation data from ArcticDEM, Polar Geospatial Center (Porter et al., 2018). Ice sheet, land, and ocean extent from Greenland Ice Sheet Mapping Project, NSIDC (Howat et al., 2014; Howat, 2017). Wind rose created from Thule Airport data covering Aug 2017-Aug 2019 (USAF, 2019).

https://doi.org/10.5194/acp-2020-340
Preprint. Discussion started: 18 May 2020

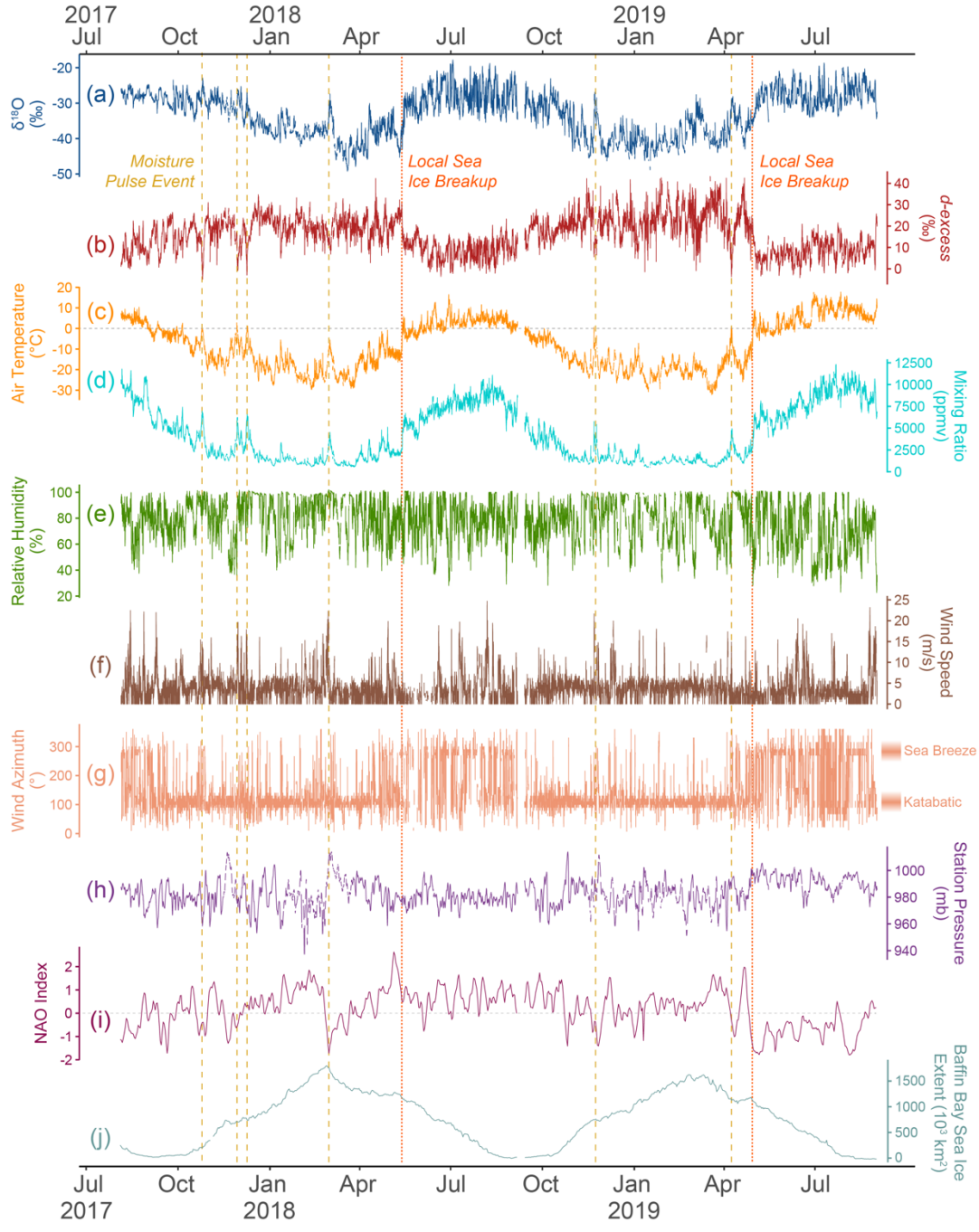

Figure 2. Observed data from Thule, Greenland, of (a) water vapor $\delta^{18}O$, (b) water vapor *d-excess*, (c) mean air temperature, (d) water vapor mixing ratio, (e) relative humidity, (f) wind speed, (g) wind azimuth, (h) station pressure, (i) NAO index (NOAA, 2019b), and (j) Baffin Bay sea ice extent (Fetterer et al., 2010). The time series of δD is very similar to $\delta^{18}O$ and not shown. Data shown here are hourly aggregations except for NAO and sea ice extent which are daily indices. All observations were taken at the South Mountain site except for wind speed and azimuth which were observed at the Thule Airport. Yellow dashed vertical lines indicate identified moisture pulse events and orange dotted vertical lines indicate the timing of sea ice breakup near Thule.

https://doi.org/10.5194/acp-2020-340
Preprint. Discussion started: 18 May 2020

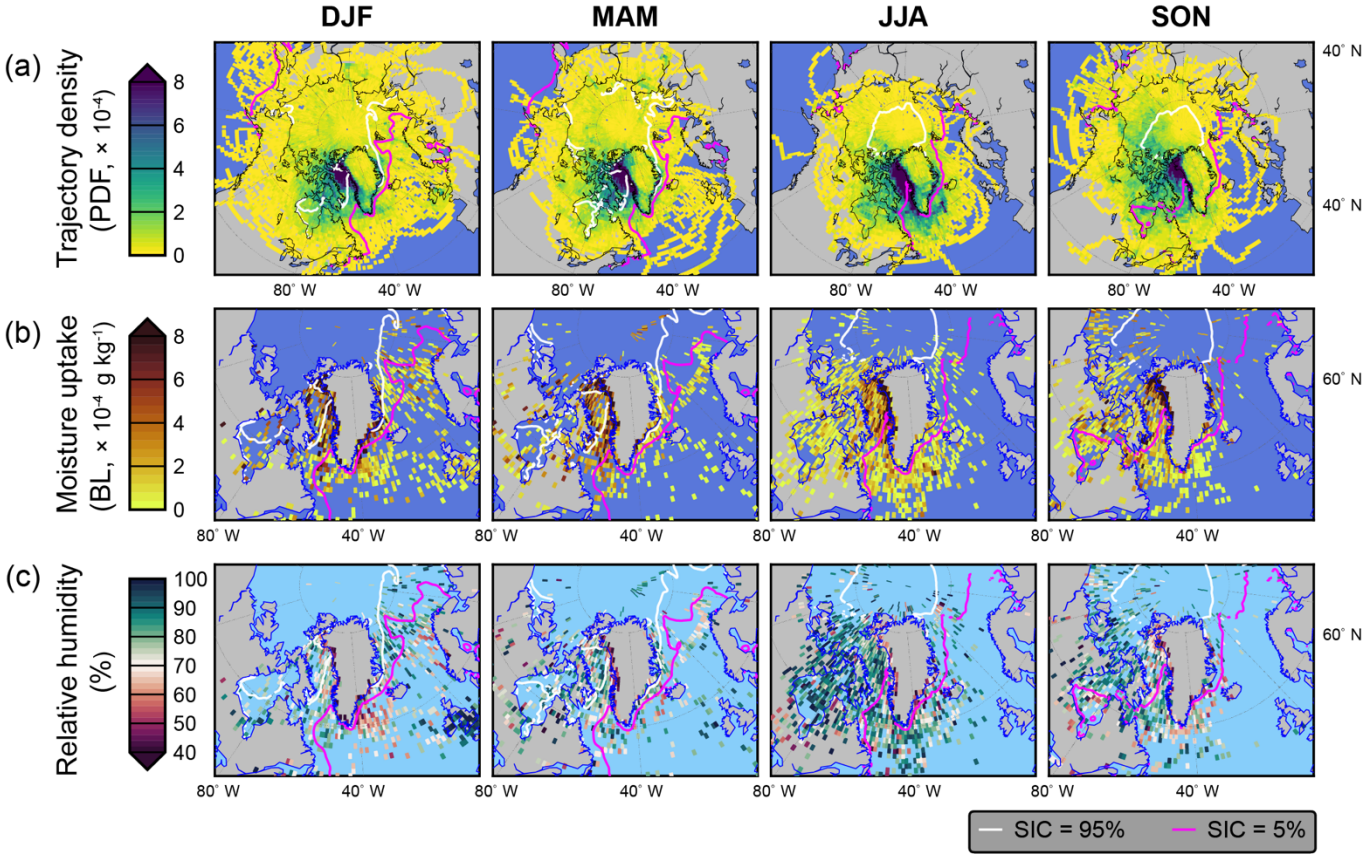

Figure 3. Back-trajectory analysis results for air parcels arriving at Thule for each meteorological season, including (a) trajectory density, (b) regions of water vapor uptake from the boundary layer (BL), and (c) relative humidity for these regions of vapor uptake. Analysis based on a quasi-climatology sampling 10 random days from each month during 1980–2018. Trajectory points are binned onto a 1-degree latitude/longitude grid as probability density functions (a) or mean values within each grid cell (b, c).

https://doi.org/10.5194/acp-2020-340
Preprint. Discussion started: 18 May 2020

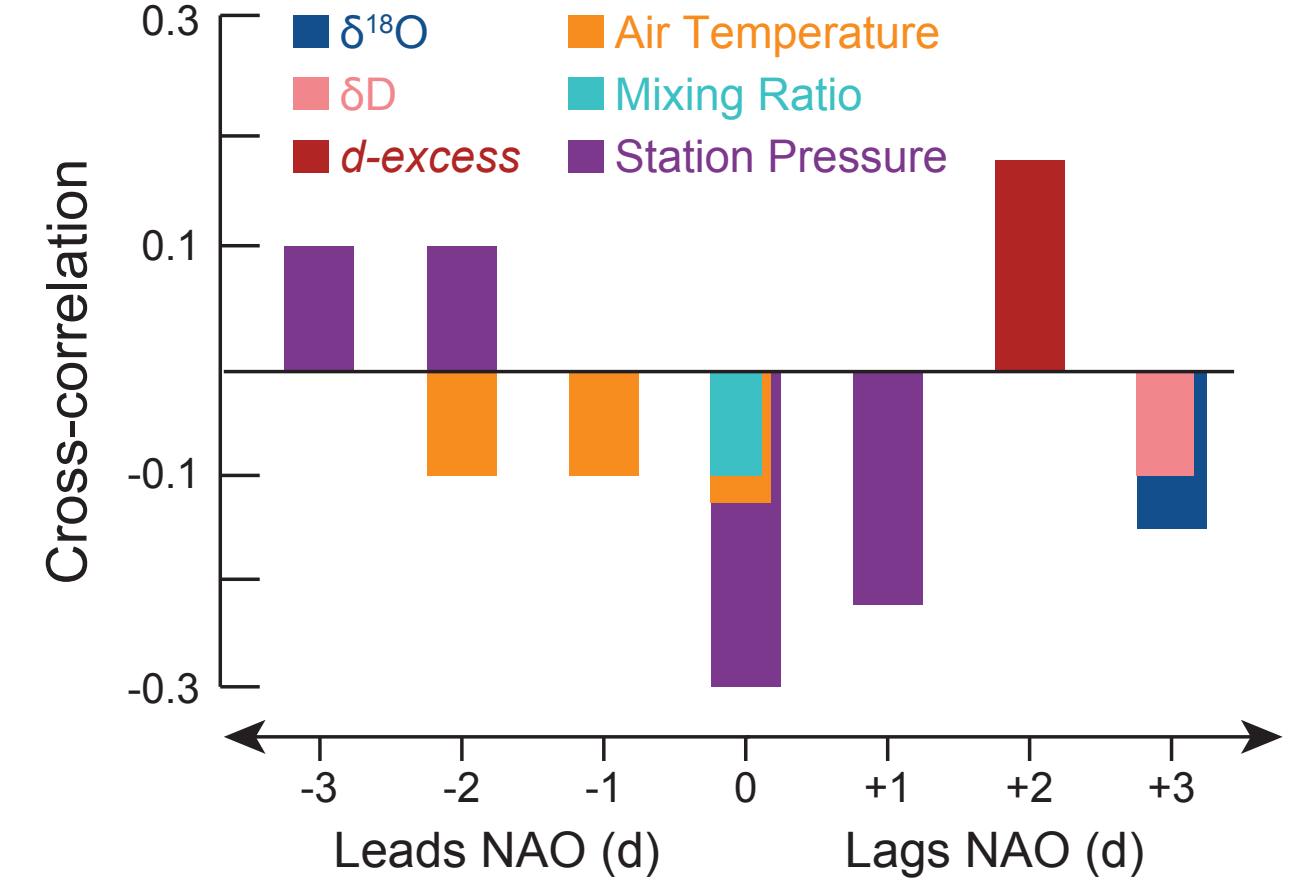

1045

Figure 4. Cross-correlation analysis results between NAO index and selected isotopic and meteorological variables. Results shown are all statistically significant at $p < 0.05$ ($n = 737$), and non-significant results are not illustrated.

https://doi.org/10.5194/acp-2020-340
Preprint. Discussion started: 18 May 2020

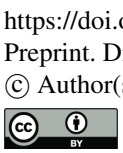

Atmospheric Chemistry and Physics Discussions

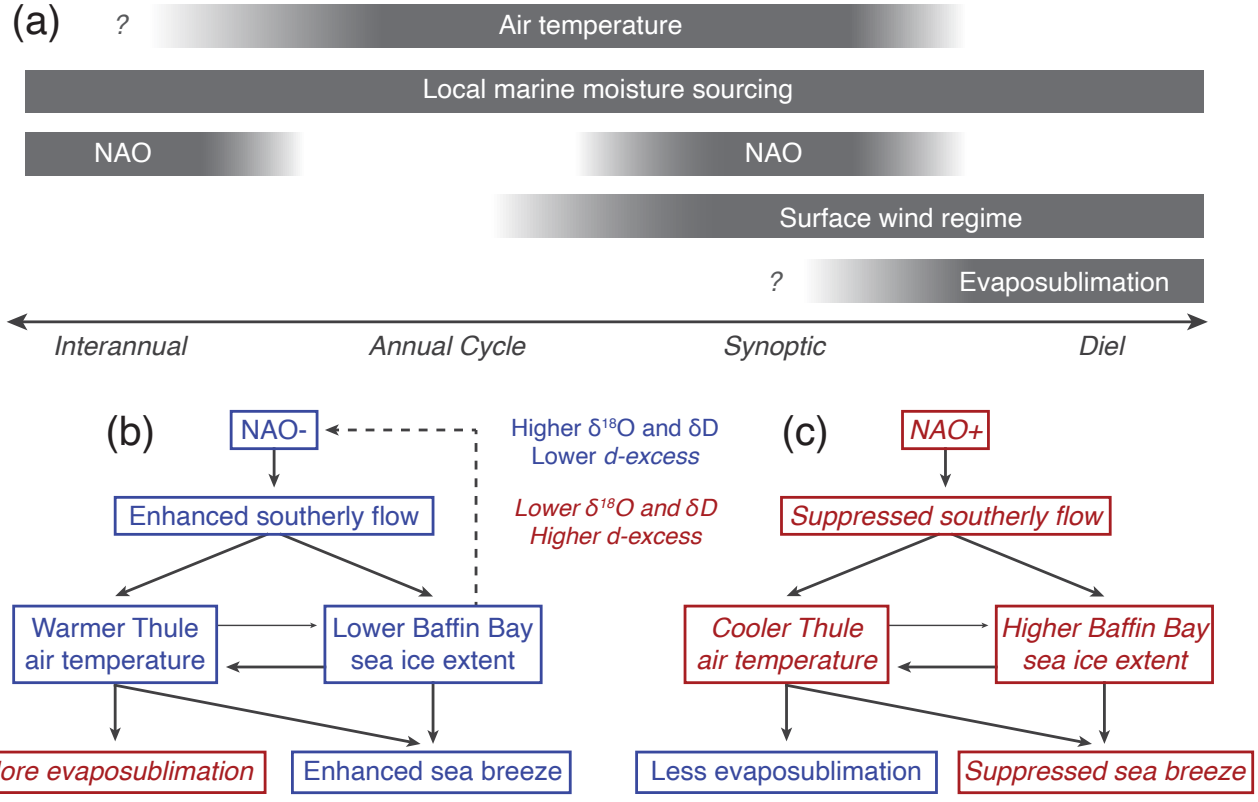

Figure 5. Summary of effects of environmental factors affecting water vapor isotope composition at Thule. (a) Illustration of temporal scales when each factor is most impactful. However, all factors can operate at any time scale. Question marks indicate periods of uncertain degree of impact. (b) Interactions between environmental factors during NAO- conditions, where factors that produce higher $\delta^{18}O$ and δD values and lower dxs values in blue, and factors that produce lower $\delta^{18}O$ and δD values and higher dxs values in italicized red. The dashed line refers to the possibility that low sea ice extent reinforces the NAO- phase (e.g., Petrie et al., 2015). (c) Same as (b), but for NAO+ conditions.

https://doi.org/10.5194/acp-2020-340
Preprint. Discussion started: 18 May 2020

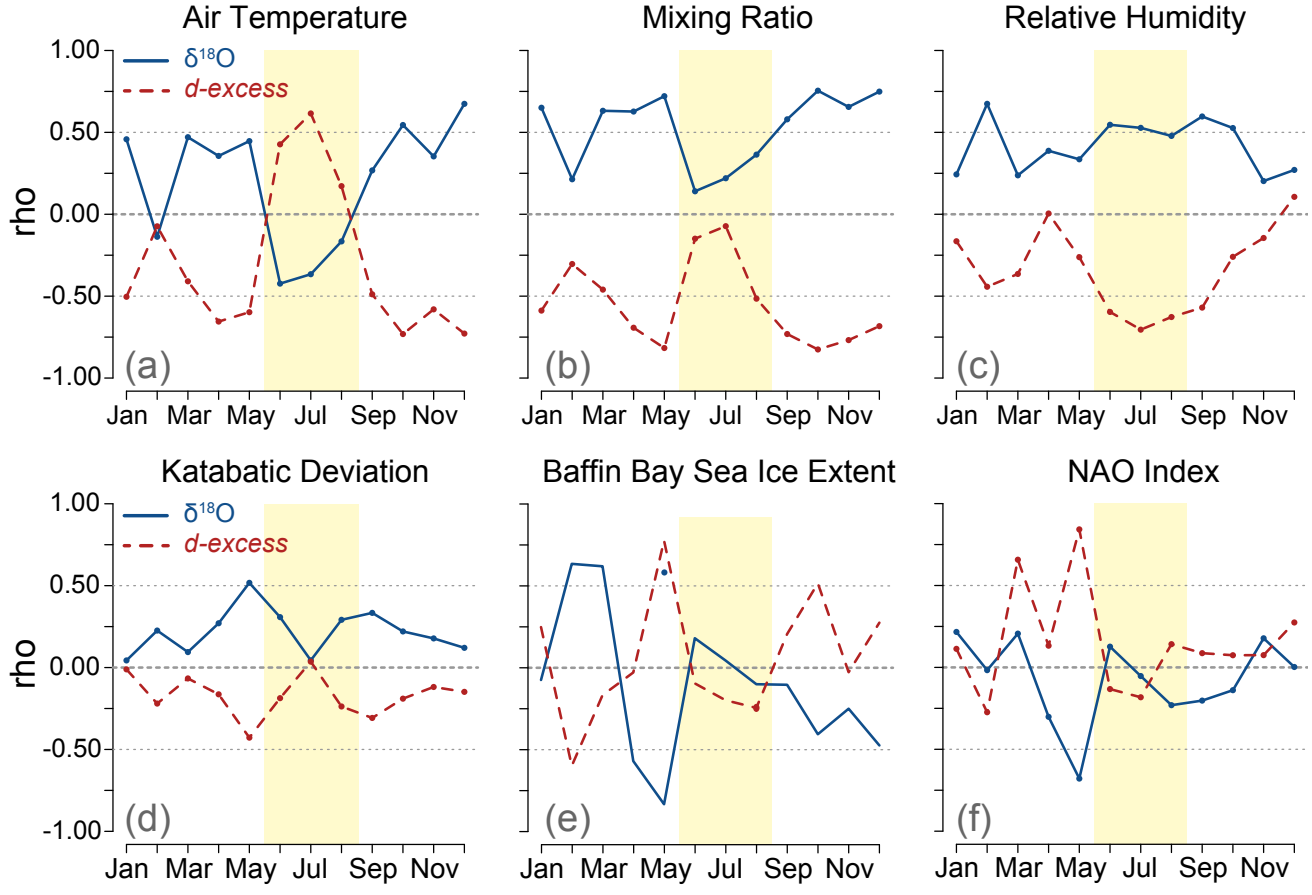

Figure 6. Spearman correlations of meteorological variables (a-f) with $\delta^{18}O$ (blue, solid) and *d-excess* (red, dashed) with data binned by month. The yellow box highlights the summer season (JJA) and horizontal dotted lines show rho values of 0.00 and ±0.50 for reference. Correlation patterns for δD (not shown) are very similar to those of $\delta^{18}O$.

https://doi.org/10.5194/acp-2020-340
Preprint. Discussion started: 18 May 2020

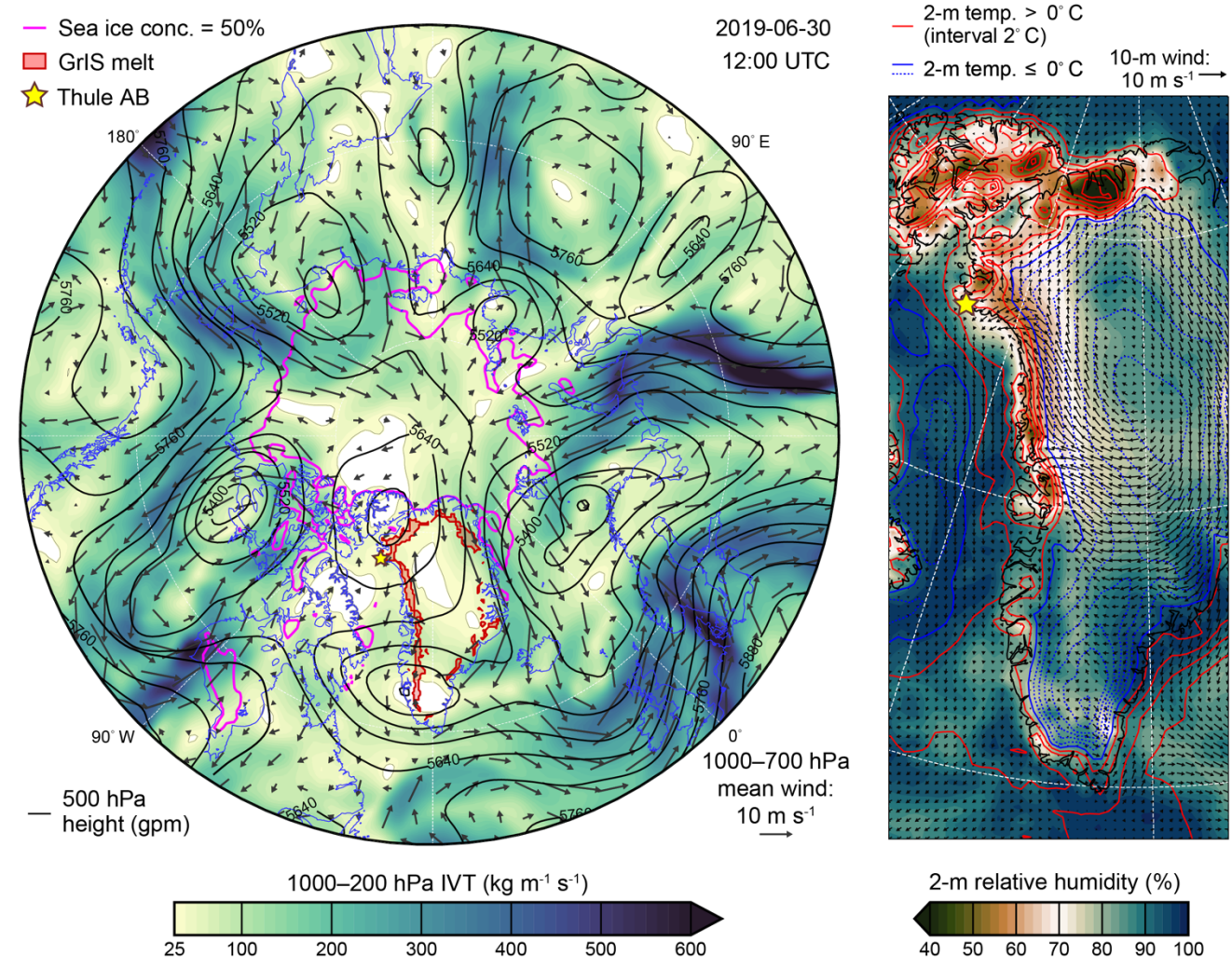

Figure 7. Synoptic (left) and local-scale (right) atmospheric conditions during an anomalously warm period on 30 June 2019, when a ridge over northwest Greenland directed downsloping air toward the observing site at Thule Air Base. Synoptic map shows integrated water vapor transport (IVT), 1000-700 hPa mean wind, 500 hPa height, as well as the 50% sea ice concentration line and areas of ice sheet surface melt. Areas in white have less than 25 kg m^{-1} s^{-1} IVT. Local scale map on right shows 2-meter relative humidity and temperature along with 10-meter wind. All data are from MERRA-2 (Stein et al., 2015; Gelaro et al., 2017) except for ice sheet surface melt, which is from the NSIDC MEaSUREs Greenland Surface Melt daily data set derived from passive microwave satellite observations (Mote, 2014).

https://doi.org/10.5194/acp-2020-340
Preprint. Discussion started: 18 May 2020

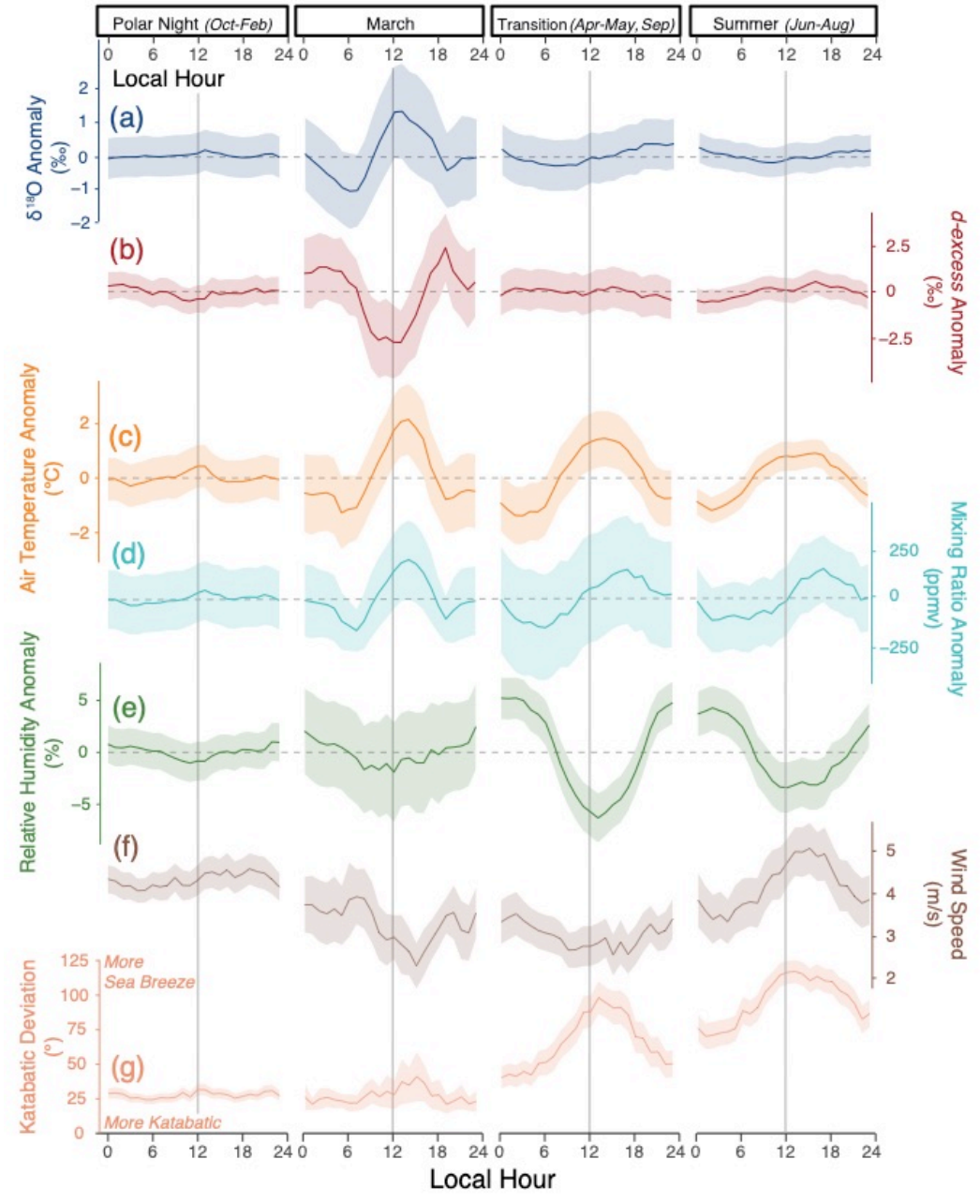

Figure 8. Diel patterns in isotopic and meteorological variables in Thule, Greenland, showing the mean hourly value (solid thick line) for each diel regime. Diel patterns for δD are very similar to $\delta^{18}O$ (a) and not shown. Colored shading indicates 95% confidence intervals for estimates of the mean. Variables other than wind speed and katabatic deviation are expressed as deviations from the mean regime value, with zero deviation shown as a dashed horizontal line. Note that because the winds in Thule are largely binary (katabatic or sea breeze), the diel means of katabatic deviations should be viewed as a probability of being katabatic or sea breeze at a given time and not that the winds are smoothly transitioning from southeast to northwest or vice versa. Additionally, because katabatic deviations increase in value both directions away from 100° (e.g., winds from 80° and 120° both have a katabatic deviation of +20°), the natural variance of purely katabatic winds produces an average value of ~25°.

https://doi.org/10.5194/acp-2020-340
Preprint. Discussion started: 18 May 2020

Atmospheric Chemistry and Physics Discussions

Table 1. Annual and seasonal mean ± 1-standard deviation values for selected water vapor isotopic and meteorological variables for Thule, Greenland, over the analytical period of this study.

	$\delta^{18}O$ (‰)	δD (‰)	*d-excess* (‰)	Air temperature (°C)	H_2O mixing ratio (ppmv)	Relative humidity (%)
Annual	-33.0±5.9	-248±41	+16.3±8.0	-8.3±11.0	4120±3020	78±17
Spring (MAM)	-35.9±5.8	-270±40	+17.7±8.5	-12.1±9.2	2850±1940	79±16
Summer (JJA)	-27.6±3.3	-212±23	+8.6±4.9	+5.3±3.9	8400±1280	73±18
Autumn (SON)	-31.1±4.1	-231±29	+17.7±5.9	-8.5±7.0	3560±1800	77±15
Winter (DJF)	-37.8±3.6	-281±26	+21.3±6.3	-18.1±5.5	1680±1010	84±16

1080